
CHALMERS
UNIVERSITY OF TECHNOLOGY

# ENGINEERING BOND MODEL FOR CORRODED REINFORCEMENT

# ENGINEERING BOND MODEL FOR CORRODED REINFORCEMENT


## ABSTRACT

Corrosion of the reinforcement in concrete structures affects their structural capacity. This problem affects many existing concrete bridges and climate change is expected to worsen the situation in future. At the same time, assessment engineers lack simple and reliable calculation methods for assessing the structural capacity of structures damaged by corrosion. This paper further develops an existing model for assessing the anchorage capacity of corroded reinforcement. The new version is based on the local bond stress-slip relationships from *fib* Model Code 2010 and has been modified to account for corrosion. The model is verified against a database containing the results from nearly 500 bond tests and by comparison with an empirical model from the literature. The results show that the inherent scatter among bond tests is large, even within groups of similar confinement and corrosion level. Nevertheless, the assessment model that has been developed can represent the degradation of anchorage capacity due to corrosion reasonably well. This new development of the model is shown to represent the experimental data better than the previous version; it yields similar results to an empirical model in the literature. In contrast to many empirical models, the model developed here represents physical behaviour and shows the full local bond stress-slip relationship. Using this assessment model will increase the ability of professional engineers to estimate the anchorage capacity of corroded concrete structures.



Keywords: Corrosion, Reinforced concrete, Anchorage, Bond, Assessment


## 1. INTRODUCTION

Many concrete structures are subjected to damaging processes, corrosion of the steel reinforcement being the most common [1]. The damage panorama ranges from corrosion in its initial stages, undetectable upon ordinary inspection, to large cracks or even spalling of the concrete cover. Climate change is expected to accelerate the deterioration, so even more severe damage over a shorter timespan may be expected in future [2]. Furthermore, demands for greater load-bearing capacity of bridges often grows with time. Thus, there is major (and increasing) demand for reliable methods to assess the capacity and remaining service life of existing infrastructure.

When reinforcement in concrete is subjected to corrosion, internal pressure is created due to the volumetric increase upon the formation of iron oxides. If the confinement of the surrounding concrete is sufficient, this may initially increase the bond capacity. As corrosion of the reinforcement bars propagates, the surrounding concrete eventually fails to carry the induced tensile stresses and longitudinal splitting cracks develop. Consequently, confinement diminishes and the bond capacity decreases [3–5]. After cracking, the capacity may either decrease markedly with further corrosion, as with minor levels of transverse reinforcement, or it may increase slightly as is the case with substantial stirrup content [6–9]. Furthermore, corrosion of reinforcement reduces the cross-sectional area of reinforcing bars, and thereby their capacity and ductility [10,11]. As many reinforcing bars have stronger steel close to the surface than in the centre of the bar, corrosion may also reduce the tensile strength of the rebar [12].

On the structural level, corrosion reduces not only the shear and moment capacity but also affects tension stiffening, and consequently the deflection and crack widths. Furthermore, plastic rotation capacity is affected. This influences moment redistribution in indeterminate structures, as well as robustness and seismic resistance [13]. In general, concrete structures are designed to show ductile failure if their ultimate capacity is exceeded, thus allowing people to avoid immediate danger. However, a corroded structure may collapse abruptly. For example, sudden bond failure in bridge beams at anchorage zones and curtailment ends can occur as a direct consequence of bond deterioration from corrosion. Reliable assessment of structural capacity is therefore particularly important.

In order to utilise the knowledge gained from previous research and advanced modelling [14,15] in engineering practice, there is a need for simplified models. These must be sufficiently accurate and time-effective for assessing existing structures. Previous work has established an analytical one-dimensional model for assessing anchorage in corroded reinforced concrete structures [16], denoted here as ARC1990. Its original formulation stems from the analytical local bond stress-slip model in Model Code 1990 [17], but has been modified based on results from a parametric study using 3D nonlinear finite element (NLFE) analyses to account for the effect of corrosion [18,19]. Subsequent verification includes a comparison with test results from naturally corroded specimens [20], a validation against 3D NLFE analyses and test results from high-level corrosion attacks that have led to cover spalling [21].

The relevance of the model in a practical context has been demonstrated in a pilot study of two bridges in Stockholm, Sweden [22]. It was shown that for these two bridges, use of the model reduced costs by approximately €3 million as unnecessary strengthening could be avoided. The Swedish Road Administration manages 20,000 bridges and there are around one million bridges in EU27, a large portion of which are made of reinforced concrete and located in corrosive environments. Considering this, the potential cost savings for society are enormous, if reliable assessment methods are made available for engineering practice.

Besides demonstrating the great capabilities of the analytical local bond model, the pilot study helped identify areas for its improvement. Areas identified as important for practical use were: incorporating the cross-sectional position of the bar being studied, and the influence of transverse reinforcement. This was enabled by implementing the *fib* Model Code 2010 [23] in the model, denoted as ARC2010. The primary aims of this paper are implementation and verification of the new model against a large bond test database of corroded specimens, plus an empirical expression.

Section 2 presents a background for assessing anchorage in corroded reinforced concrete and a comparison between local bond stress-slip relationships in *fib* Model Code 1990 and 2010. There is also a description of ARC2010, the proposed engineering bond model for corroded reinforcement. Section 3 presents a collection of bond tests of corroded specimens, plus calibration and verification of the proposed bond model. The results are discussed in Section 4, and conclusions and an outlook are given in Section 5.

# 2. A PROPOSED ENGINEERING BOND MODEL

## 2.1. Assessment of anchorage in corroded RC structures

Analytical procedures for assessing anchorage capacity and other aspects of structural behaviour can differ in complexity, depending on the extent to which actual physical behaviour is to be captured. Ideally, a

more complex analysis should mean improved representation of actual behaviour in comparison with a simpler analysis. However, the cost in terms of an analyst's time and expertise will be higher.

### 2.1.1 Different levels of assessment

The level of detail in a structural assessment can be divided into several categories. This approach is based on the principle of successively improved evaluation in structural assessment and comprises four different assessment levels [24], level I being the simplest and level IV the most advanced. A description of the assessment levels is presented in Figure 1.

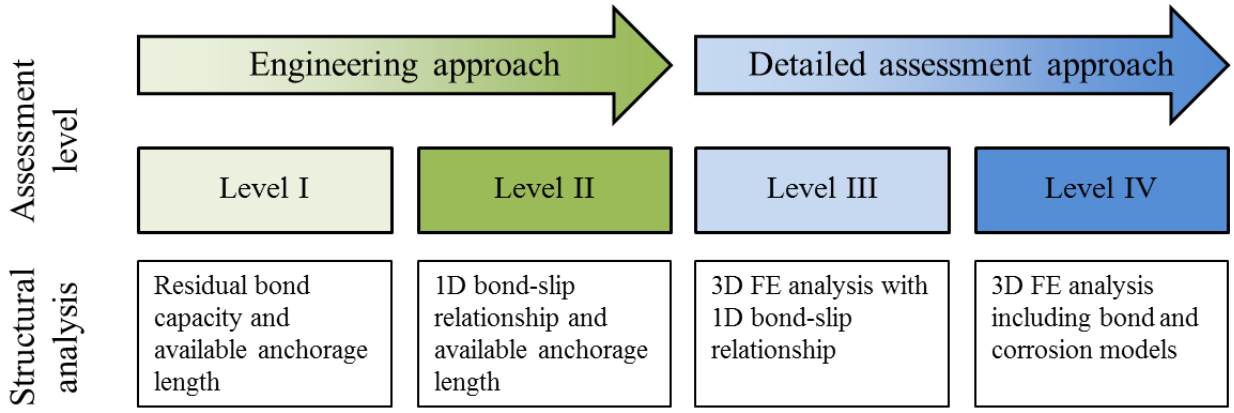


*Figure 1: Description of assessment levels I to IV for the assessment of anchorage capacity in reinforced concrete with corroded reinforcement, proposed by and adopted from* [24].

Assessment levels I and II are strength based and one dimensional (1D) approaches, respectively. These do not require a non-linear finite element (NLFE) analysis and are considered suitable for application in engineering practice. In level I assessments, only the residual capacity given by the local bond stress-slip relationship is considered over an assumed anchorage length. In the more refined level II approach, the entire local bond stress-slip relationship is used to solve the 1D differential equation over the available anchorage length and obtain the anchorage capacity. Levels III and IV require the use of NLFE analyses. The main difference is that in level III the interaction between reinforcement bars and concrete is treated using local bond stress-slip relation, whilst in level IV the interaction is explicitly represented by models describing the bond action, cf. Lundgren 2005a [25] and models accounting for the influence of corrosion, cf. Lundgren 2005b [26], applied to the interface between reinforcement bars and concrete. The latest developments include advanced models for the interaction between mechanical and non-mechanical effects of corrosion, cf. Ožbolt et al. [27]. In this paper, the assessment of anchorage has been carried out according to assessment level II. A more detailed description of this level is presented in the following section.

### 2.1.2 Description of anchorage assessment level II

In assessments at level II, the force that can be anchored is calculated by solving the equilibrium conditions along the reinforcement bar. The differential equation [16] is:

$$\frac{\pi \cdot \phi_m{}^2}{4} \cdot \frac{d\sigma_s}{dx} - \pi \cdot \phi_m \cdot \tau_b = 0 \qquad (1)$$

where $\phi_m$ is the reinforcement diameter, $\sigma_s$ is the stress in the reinforcement and $\tau_b$ is the local bond stress. The reinforcement bar within the anchorage length is assumed to be in the elastic range, thus:

$$\sigma_s = E_s \varepsilon_s, \quad \varepsilon_s = \frac{du}{dx} \tag{2, 3}$$

where $E_s$ is the elastic modulus, $\varepsilon_s$ is the strain and $u$ denotes the displacement of the reinforcement bar. The bond stress $\tau_b$ is defined by the local bond stress-slip relation. For an uncorroded case, the local-bond slip relationship from, say, Model Code 2010 [23] can be used to assess the anchorage. For a corroded bar, modified local bond stress-slip curves as suggested in this paper can be used; see Section 2.3. If the deformation of the surrounding concrete is neglected, the slip, $s$, equals the displacement of the rebar:

$$u = s \tag{4}$$

When considering pull-out of a reinforcement bar with embedment length $l_b$ and prescribed displacement $u_{l_b}$, the boundary conditions are:

$$\sigma_s(0) = 0, \quad u(l_b) = u_{l_b} \tag{5, 6}$$

The differential equation can be solved numerically to obtain the steel stress and deformation along the rebar, and accordingly also the pull-out force and average bond stress over the embedment length.

## 2.2 Comparison of local bond stress-slip relationships in Model Code 1990 and 2010

The difference between the local bond stress-slip relationships from the two versions of Model Code and the resulting influence when used in a level II assessment are presented in Sections 2.2.1 and 2.2.2 respectively.

### 2.2.1 Original local bond stress-slip relationships in Model Codes 2010 and 1990

The analytical one-dimensional model for the assessment of anchorage in corroded reinforced concrete structures in [16] was based on the local bond stress-slip relationship in Model Code 1990 [17]. There, the confinement conditions are defined as either “confined” or “unconfined”, corresponding to pull-out and splitting failure respectively. Interpolation between these cases can be carried out based on concrete cover to bar diameter ratio and stirrup content.

In Model Code 2010, the local bond strength corresponding to splitting of the specimen is calculated explicitly; this governs the local bond stress-slip relation, if it is smaller than the pull-out strength [23]. The local bond strength expressions in Model Codes 1990 and 2010 have a common feature in the differentiation between “Good bond conditions” and “All other bond conditions”. “Good bond conditions” applies to all bars with 45-90° inclination to the horizontal during concreting as well as those with less than 45° to the horizontal, which are up to 250 mm from the bottom, or at least 300 mm from the top, of the concrete layer during concreting.

In both Model Codes 1990 and 2010, “All other bond conditions” means a reduction of maximum local bond strength. For Model Code 2010, the splitting strength is also reduced compared with “Good bond conditions”. For monotonic loading, the local bond stresses can be calculated as a function of the relative displacement according to Equations 7-10, which are common to Model Codes 1990 and 2010:

$$\tau_b = \tau_{bmax}(s/s_1)^{\alpha} \quad \text{for } 0 \le s \le s_1 \qquad (7)$$

$$\tau_b = \tau_{bmax} \quad \text{for } s_1 \le s \le s_2 \qquad (8)$$

$$\tau_b = \tau_{bmax} - (\tau_{bmax} - \tau_{res})\,(s - s_2)/(s_3 - s_2) \quad \text{for } s_2 \le s \le s_3 \qquad (9)$$

$$\tau_b = \tau_{res} \quad \text{for } s_3 \le s \qquad (10)$$

where the parameters for Model Codes 2010 and 1990 are given for pull-out failure and splitting failure in Table 1 and Table 2 respectively.

*Table 1: Parameters defining local bond stress-slip curve for pull-out failure for Model Codes 2010 and 1990.*

| | **Pull-out (MC 2010)** | | **Pull-out (MC 1990)** | |
|---|---|---|---|---|
| | **"Good"** | **"All other"** | **"Good"** | **"All other"** |
| $\boldsymbol{\tau_{bmax}}$ | $2.5\sqrt{f_{cm}}$ | $1.25\sqrt{f_{cm}}$ | $2.5\sqrt{f_{ck}}$ | $1.25\sqrt{f_{ck}}$ |
| $\boldsymbol{s_1}$ | 1.0 $mm$ | 1.8 $mm$ | 1.0 $mm$ | 1.0 $mm$ |
| $\boldsymbol{s_2}$ | 2.0 $mm$ | 3.6 $mm$ | 3.0 $mm$ | 3.0 $mm$ |
| $\boldsymbol{s_3}$ | ${c_{clear}}^{\star}$ | ${c_{clear}}^{\star}$ | ${c_{clear}}^{\star}$ | ${c_{clear}}^{\star}$ |
| $\boldsymbol{\alpha}$ | 0.4 | 0.4 | 0.4 | 0.4 |
| $\boldsymbol{\tau_{res}}$ | $0.4\tau_{bmax}$ | $0.4\tau_{bmax}$ | $0.4\tau_{bmax}$ | $0.4\tau_{bmax}$ |

$^{\star}$ $c_{clear}$ is the clear distance between ribs.

*Table 2: Parameters defining local bond-slip curve for splitting failure for Model Codes 2010 and 1990.*

| | **Splitting (MC 2010)** | | | | **Splitting (MC 1990)** | |
|---|---|---|---|---|---|---|
| | **"Good"** | | **"All other"** | | **"Good"** | **"All other"** |
| | **Unconfined** | **Stirrups** | **Unconfined** | **Stirrups** | | |
| $\boldsymbol{\tau_{bmax}}$ | $2.5\sqrt{f_{cm}}$ | $2.5\sqrt{f_{cm}}$ | $1.25\sqrt{f_{cm}}$ | $1.25\sqrt{f_{cm}}$ | $2.0\sqrt{f_{ck}}$ | $1.0\sqrt{f_{ck}}$ |
| $\boldsymbol{\tau_{bu,split}}$ | Eq. 11 | Eq. 11 | Eq. 11 | Eq. 11 | - | |
| $\boldsymbol{s_1}$ | $s(\tau_{bu,split})$ | $s(\tau_{bu,split})$ | $s(\tau_{bu,split})$ | $s(\tau_{bu,split})$ | 0.6 $mm$ | 0.6 $mm$ |
| $\boldsymbol{s_2}$ | $s_1$ | $s_1$ | $s_1$ | $s_1$ | 0.6 $mm$ | 0.6 $mm$ |
| $\boldsymbol{s_3}$ | $1.2s_1$ | ${0.5c_{clear}}^{\star}$ | $1.2s_1$ | ${0.5c_{clear}}^{\star}$ | 1.0 $mm$ | 2.5 $mm$ |
| $\boldsymbol{a}$ | 0.4 | 0.4 | 0.4 | 0.4 | 0.4 | 0.4 |
| $\boldsymbol{\tau_{res}}$ | $0^{\dagger}$ | ${0.4\tau_{bu,split}}^{\dagger}$ | $0^{\dagger}$ | ${0.4\tau_{bu,split}}^{\dagger}$ | $0.15\tau_{bmax}$ | $0.15\tau_{bmax}$ |

$^{\star}$ $c_{clear}$ is the clear distance between ribs.

$^{\dagger}$ residual capacity modified in the proposed model, ARC2010.

The splitting strength is estimated in Model Code 2010 as:

$$\tau_{bu,split} = \eta_2 \cdot 6.5 \cdot \left(\frac{f_{cm}}{25}\right)^{0.25} \cdot \left(\frac{25}{\phi_m}\right)^{0.2} \left[\left(\frac{c_{min}}{\phi_m}\right)^{0.25} \left(\frac{c_{max}}{c_{min}}\right)^{0.1} + k_m \cdot K_{tr}\right] \qquad (11)$$

where $\eta_2$ is 1.0 and 0.7 for "good" and "all other" bond conditions respectively; $f_{cm}$ is the mean cylinder compressive strength in MPa; $\phi_m$ is the diameter of the anchored bar in mm; $c_{min}$ and $c_{max}$ are given in

Equations 12 and 13; $k_m$ and $K_{tr}$ are the confinement coefficient and the amount of the transverse reinforcement respectively. It should be noted that Equation 11 assumes a constant bond stress over a bonded length of five times the diameter of the anchored bar, i.e. a local bond stress-slip relationship is considered. To obtain the average bond strength over a longer embedment length the differential Equation 1 should be solved.

$$c_{min} = \min\left(c_s/2\,, c_x, c_y\right) \tag{12}$$

$$c_{max} = \max(c_s/2\,, c_x) \tag{13}$$

where $c_s$ is the clear spacing between main bars; $c_x$ is the cover in *x*-direction and $c_y$ is the cover in *y*-direction; $k_m = 12$ for bars located within $5\phi_m \leq 125\ mm$ from a stirrup corner, $k_m = 6$ if $c_s > 8c_y$ or $k_m = 0$ if $c_s < 8c_y$, or if a crack can propagate to the concrete surface without crossing transverse links.

The transverse reinforcement is quantified as:

$$K_{tr} = n_t A_{st}/(n_b \phi_m s_t) \leq 0.05 \tag{14}$$

where $n_t$ is the number of legs of confining reinforcement crossing a potential splitting-failure surface at a section, $A_{st}$ is the cross-sectional area of one leg of a transverse bar, $s_t$ is the longitudinal spacing of confining reinforcement and $n_b$ is the number of anchored bars or pairs of lapped bars in the potential splitting surface.

For comparison, some examples of the local bond stress-slip curves from Model Codes 2010 and 1990 are presented in Figure 2. These examples use C50/60 concrete, "Good bond conditions", $\phi_m = 20\ mm$, with cover $c = 2\phi$. The stirrup amount is $K_{tr} = 0.05$ (if applicable) with effectiveness factor $k_m = 12$. The clear spacing between ribs is chosen to $c_{clear} = 5.8\ mm$ and the inclining branch shape factor $\alpha = 0.4$. It should be noted that in Model Code 1990, the "Splitting" case requires a minimum amount of transverse reinforcement equivalent to 25% of the longitudinal reinforcing steel in the cross section; also, linear interpolation is allowed between the "Pull-out" and "Splitting" cases.

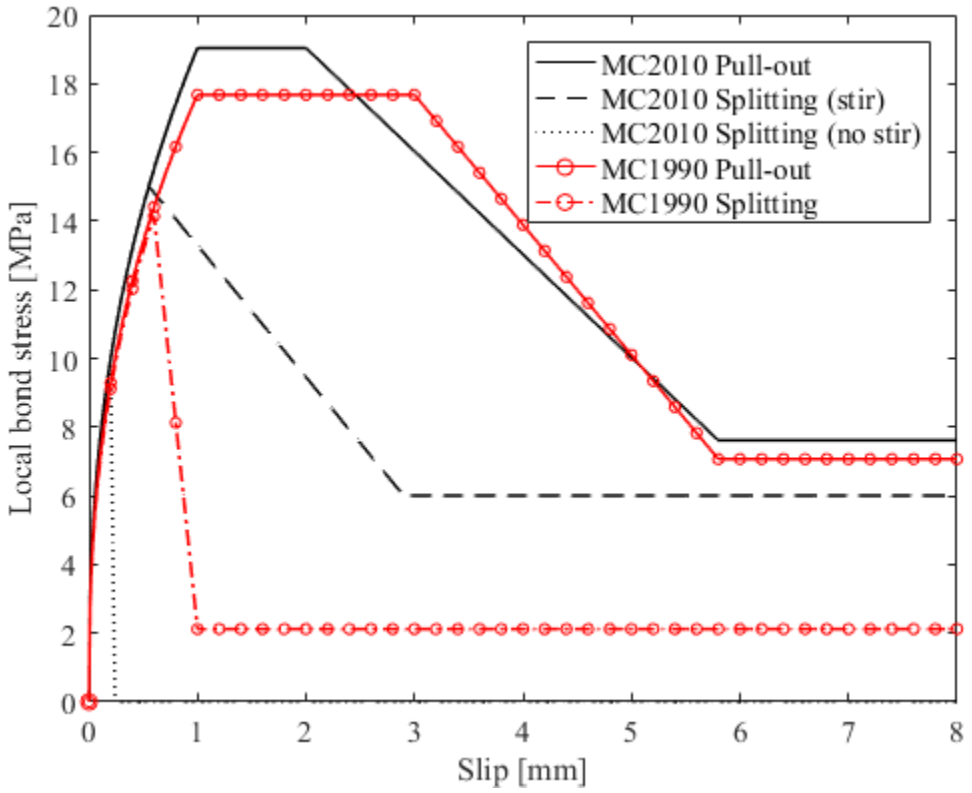


*Figure 2: Comparison of the local bond stress-slip expressions for "Good bond conditions" in Model Codes 2010 and 1990, C50/60 concrete,* $\phi_m = 20\,mm$, $k_m = 12$, $K_{tr} = 0.05$, $c = 40\,mm$, $c_{clear} = 5.8\,mm$ *and* $\alpha = 0.4$.

### 2.2.2 Comparison of average bond strength from level II analysis using Model Codes 2010 and 1990

The anchorage capacities of Model Codes 2010 and 1990 when used in level II analyses are investigated via the statistical method "*factorial design*", see [28]. This allows for a structured, quantitative comparison of the average bond strength (calculated as the pull-out force divided by the rebar surface area along the embedment length) as well as the influence of input parameters, which may differ between the models.

In principle, the method is simple: the input parameters (independent variables) for the models are assigned two levels (two discrete values) denoted "–" and "+". For example, reinforcement diameters can have a "–" level of 16 mm and a "+" level of 20 mm. Then the response variable (dependent variable), the average bond strength in this case, is calculated for all possible combinations of "–" and "+" levels. The required number of calculations is $2^k$, when two levels are considered for each input parameter and where $k$ is the number of input parameters.

Model Code 2010 and 1990 are compared for the case of a reinforcement bar being close to an edge, i.e. markedly thicker concrete cover in the horizontal direction compared to the vertical direction. Eight and five input parameters are considered for the cases with and without stirrups, respectively. The input parameters for the factorial design are presented in Table 3.

*Table 3: Input parameter levels for Model Codes 1990 and 2010 in factorial design.*

| Input parameters | Parameter levels with stirrups | | Parameter levels without stirrups | |
|---|---|---|---|---|
| | – | + | - | + |
| Main bar diameter $\phi_m$ [mm] | 16 | 20 | 16 | 20 |
| Cover $y$-dir $c_y$ [mm] | 20 | 60 | 20 | 60 |
| Concrete compressive strength $f_{cm}$ [MPa] | 38 | 48 | 38 | 48 |
| Young's modulus $E_s$ [GPa] | 190 | 210 | 190 | 210 |
| Yield strength main bars $f_y$ [MPa] | 450 | 550 | 450 | 550 |
| Stirrup diameter $\phi_s$ [mm] | 6 | 12 | - | - |
| c-c stirrups $s_t$ [mm] | 50 | 200 | - | - |
| Yield strength stirrups $f_{yt}$ [MPa] | 450 | 550 | - | - |

A bonded length of five times the main bar diameter is used, i.e. either 80 mm or 100 mm. The cover in the x-direction, i.e. horizontal, is 150 mm to represent a bar relatively far away from a corner. The average bond strength for all possible combinations (i.e. $2^8 = 256$ and $2^5 = 32$) is calculated by level II analyses using the local bond stress-slip relationships of Model Codes 2010 and 1990. For the case with stirrups, the stirrup content is accounted for by a linear interpolation between "Confined" and "Unconfined" cases in Model Code 1990, but is included in the expression of splitting strength (see Equation 11) in Model Code 2010.

The main effect ($ME$) of an input parameter is computed as the difference between the average value of all results for the two different parameter levels. Thus, the main effect of input parameter $n$ can be written:

$$ME_n = \overline{y}_n^+ - \overline{y}_n^- \quad (15)$$

where $\overline{y}_n^+$ and $\overline{y}_n^-$ are the average responses (average bond strength) of all calculations where parameter $n$ was assigned its "+" and "–" levels respectively.

Figure 3 shows the differences of resulting average bond strengths and influence of input parameters between Model Codes 1990 and 2010, when applied in level II analyses. The left and right ends of the lines indicate $\overline{y}_n^-$ and $\overline{y}_n^+$ respectively and therefore the slope indicates the main effect of the parameter. It should be noted that these main effects are valid within the studied parameter ranges but may differ if other values are selected for the "–" and "+" levels of the input parameters.

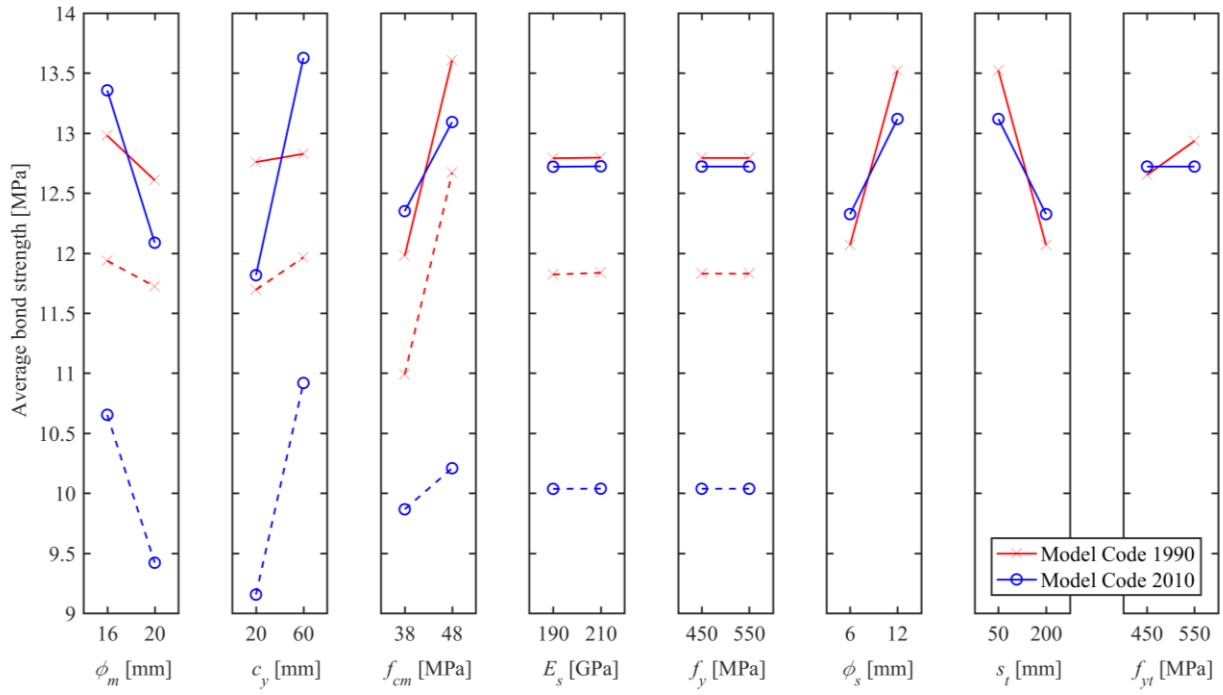


*Figure 3: Comparison between Model Code 2010 and Model Code 1990 results from level II analysis. The inclination of the lines is interpreted as the influence of the corresponding input parameter. The solid lines and dashed lines represent cases with stirrups and without stirrups, respectively.*

Firstly, it is concluded from the overview of all parameters that Model Code 2010 predicts a lower average bond strength than Model Code 1990; the difference is large for cases without stirrups. This difference is due to that the residual branch of the local bond stress-slip relationship is zero for cases without stirrups in Model Code 2010, while a small capacity remains in the 1990 version. This leads to a smaller anchorage capacity when the differential equation (Equation 1) is solved over the bonded length.

Secondly, an increase of the main bar diameter gives a more pronounced reduction in Model Code 2010, similarly an increase of concrete cover $c_y$ is also more influential compared to in Model Code 1990. This is because both $\phi_m$ and $c_y$ are influential parameters in the expression for the splitting strength in Model Code 2010.

Since the concrete compressive strength directly determines the maximum local bond capacity in Model Code 1990, while the splitting strength often governs in Model Code 2010, a greater influence from the concrete compressive strength is anticipated in MC1990.

The influence of stirrup diameter and spacing is relatively similar for both versions of Model Code, however it is a bit more pronounced in the 1990 version.

As expected, the properties of the main reinforcement steel do not influence the average bond strength capacity. This is because the embedment lengths (chosen for both parameter levels) are short and consequently the steel does not yield. However, the strength of the transverse reinforcement influences the

capacity in Model Code 1990, since it is included in the interpolation between "Confined and "Unconfined" case.

## 2.3 Proposed new model for anchorage assessment in concrete structures with corroded reinforcement

The proposed model for the assessment of Anchorage in corroded Reinforced Concrete structures (ARC2010) is based on the local bond stress-slip relationship in Model Code 2010 [23]. The proposed model includes the following modified and additional elements so as to account for the effect of corrosion:

- Introduction of equivalent slip to account for bond degradation due to corrosion.
- Change of failure mode due to corrosion-induced cracking of the concrete cover.
- Modification of residual bond stress in case of low stirrup content.

### 2.3.1 Equivalent slip to account for the effect of corrosion

It has previously been observed that the local bond stress-slip curve of corroded reinforcement can be approximated by shifting the uncorroded curve in the slip direction [18,19]. The local bond stress-slip curve for corroded reinforcement is then obtained as the minimum bond stress value of the original and the shifted curve. In other terms, the approximation means that corrosion exhausts the bond capacity in a similar manner to slip. This principle is illustrated in Figure 4.

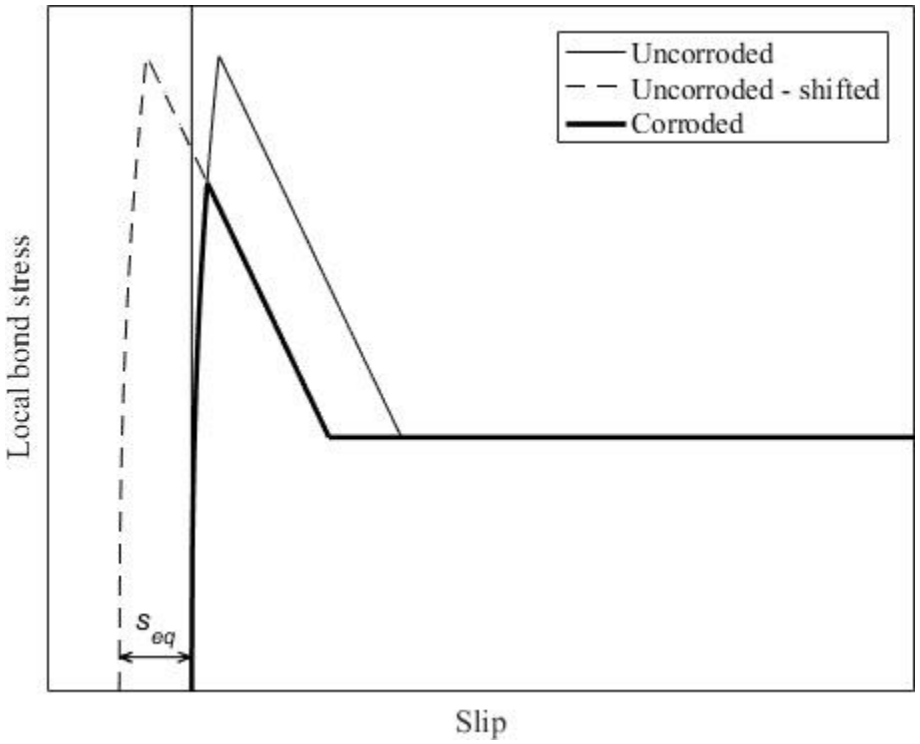


*Figure 4: Illustration of the equivalent slip, $s_{eq}$, to account for the effect of corrosion in a local bond stress-slip curve, where splitting strength governs the maximum bond stress.*

As stated previously, the reduction in capacity due to corrosion is accounted for by shifting the local bond-slip curve, i.e. an equivalent slip added to the slip between steel and concrete. This can be expressed as:

$$s_{eff} = s + s_{eq} \quad (16)$$

where $s_{eff}$ is the effective slip, $s$ is the mechanical slip and $s_{eq}$ is the equivalent slip to account for the effect of corrosion.

To illustrate the principle in an actual example, the average bond stress-slip curve from uncorroded test results in Lin & Zhao 2016 [29] is plotted together with results from a corroded specimen in the same experimental campaign in Figure 5. The curve from the uncorroded test shifted in the slip direction is also plotted. An equivalent slip of $s_{eq} = 1.68\,mm$ was applied, obtained from the expression calibrated in Section 3.2. As can be seen in Figure 5, this yields similar peak bond strength as in the bond stress-slip curve of the corroded specimen, and the descending branch and residual strength are reasonably well captured. Note that in this example, the average bond stress calculated as the pull-out force divided by the rebar surface area along the embedment length was used, even though the model is meant to be applied to the local bond stress. Here, the intention was only to show the principle of equivalent slip applied to experimental results directly.

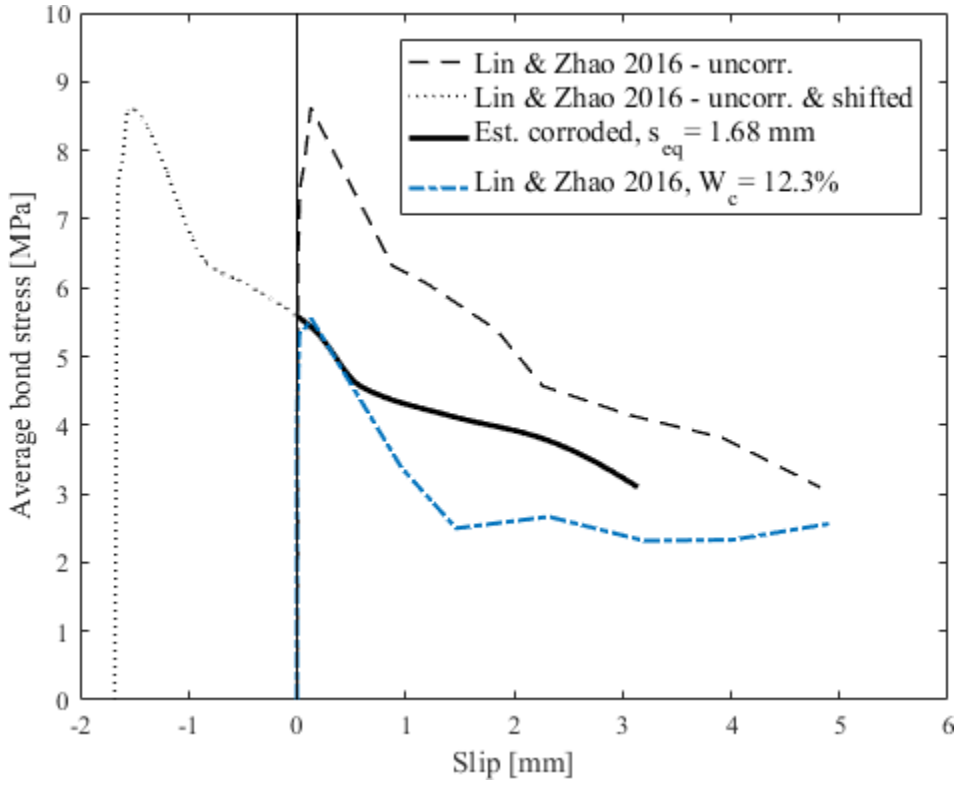


*Figure 5: Illustration of the procedure for applying an equivalent slip, i.e. shifting the average bond stress-slip curve in the direction of slip;$s_{eq}$ is the equivalent slip and $W_c$ is the corrosion level.*

### 2.3.2 Influence of corrosion-induced cracks

Increasing corrosion levels will ultimately crack the concrete cover. The corrosion penetration leading to cracking can, according to [16], be estimated as:

$$x_{cr} = 11 \cdot \left(\frac{f_{cm}}{40}\right)^{0.8} \cdot \left(\frac{c}{\phi_m}\right)^{1.5} \cdot \left(\frac{\phi_m}{16}\right)^{0.5} \quad (17)$$

where $f_{cm}$ is the concrete cylinder compressive strength in MPa, $c$ the concrete cover and $\phi_m$ the rebar diameter, all in mm. This expression was found by curve-fitting 3D analyses, assuming uniformly distributed corrosion. The influence of corrosion distribution will be discussed further in Section 4.2. Through geometric observation the corresponding corrosion level in terms of weight loss, $W_{cr}$, can be calculated based on the corrosion penetration.

The original splitting strength is used for corrosion levels below cracking limit, see Equation 11. However, when the concrete cover is cracked by corrosion, the confinement provided by that cover is decreased. It is suggested to account for this by reducing the factor for concrete cover to 1, thus obtaining the reduced splitting strength:

$$\tau_{bu,split,red} = \eta_2 \cdot 6.5 \cdot \left(\frac{f_{cm}}{25}\right)^{0.25} \cdot \left(\frac{25}{\phi_m}\right)^{0.2} (1 + k_m \cdot K_{tr}) \quad (18)$$

where $\eta_2$ is 1.0 and 0.7 for "Good bond conditions" and "All other bond conditions" respectively, $f_{cm}$ is the mean cylinder compressive strength, $\phi_m$ is the diameter of the anchored bar being considered, $k_m$ is a confinement coefficient and $K_{tr}$ is the amount of transverse reinforcement. Similar to Equation 11, the above expression is based on an embedment length of five times the bar diameter and is used to obtain the local bond stress-slip curve for cases where the cover is cracked.

If the concrete is confined enough to exhibit a pull-out failure mode in the uncorroded case, then a corrosion level leading to cracking of the concrete cover will change the failure mode. In ARC2010, this is represented by changing the local bond stress-slip behaviour from pull-out to splitting upon corrosion-induced cracking. The splitting strength is calculated using Equation 18. The same applies to cases where splitting governs the failure in the uncorroded case. Accordingly, the reduced splitting strength after cracking of the concrete cover is also obtained by Equation 18.

For cases with stirrups, the slip level at the maximum local bond stress $s_1$ is calculated based on the reduced splitting strength; the residual is reached for slip level $s_3$ of $0.5\ c_{clear}$.

For cases without stirrups, $s_1$ (equal to $s_2$) is increased by 25% to avoid overly narrow peaks in the local bond stress-slip relationship. $s_3$ is computed as $1.2s_1$, as given in Model Code 2010. Local bond stress-slip curves for un-cracked cases and cases cracked by corrosion are presented in Figure 6. Note that the equivalent slip, as presented in Section 2.3.1, is used to account for different levels of corrosion, and the change in failure mode between cracked and un-cracked cases presented here is used to give a distinct change in capacity between the two cases.

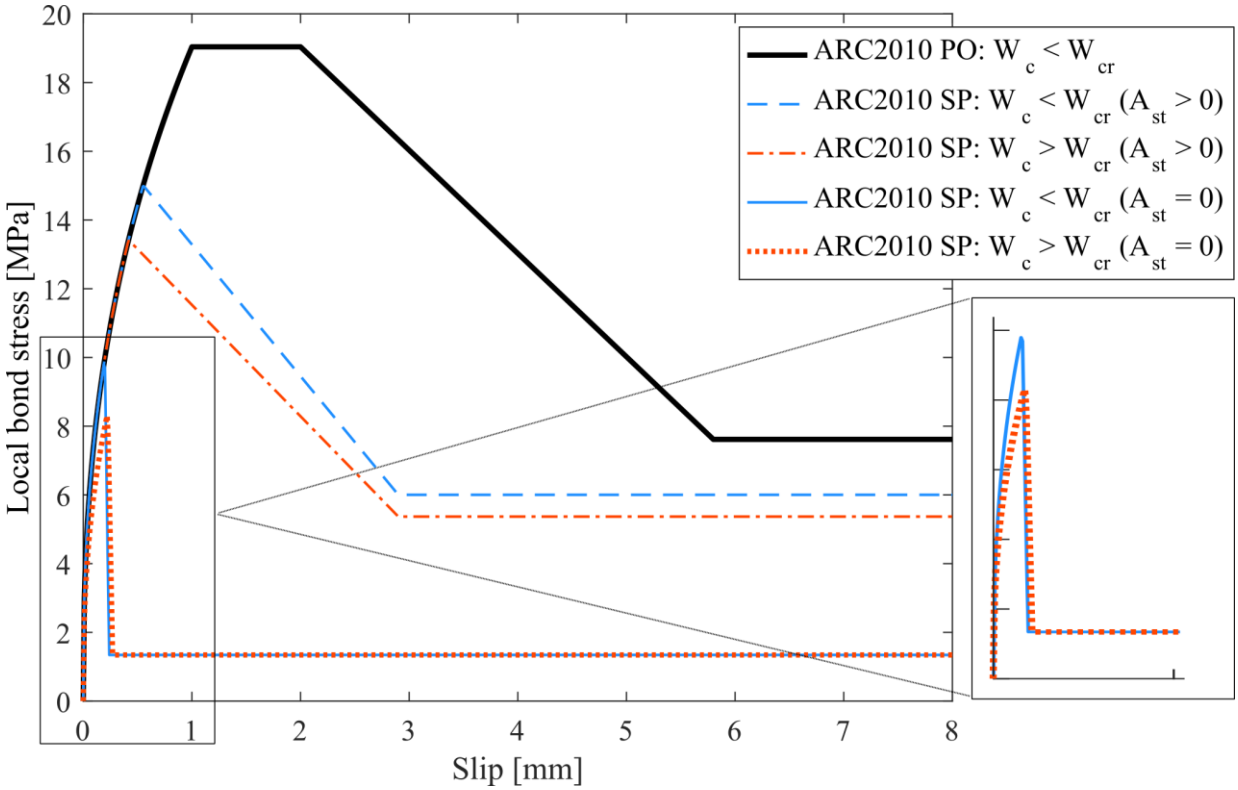


*Figure 6: Change from pull-out failure to splitting failure due to corrosion for "Good bond conditions", C50/60 concrete, $\phi_m = 20\ mm$, $k_m = 12$, $K_{tr} = 0.05$, $c = 40\ mm$, $c_{clear} = 5.8\ mm$ and $\alpha = 0.4$. PO indicates pull-out failure and SP indicates splitting.*

### 2.3.3 Modification of residual capacity

In Model Code 2010, the capacity after splitting (residual bond stress) is zero if no transverse reinforcement is present. By applying a slip equivalent to a high corrosion level, the bond capacity would thus become zero. Nevertheless, several researchers have reported normalised bond strengths of 10-60% [15,30,31] from tests on specimens with high levels of corrosion (>10%, artificial corrosion), relatively small concrete cover ($< 2\ \phi_m$) and no transverse reinforcement. In the light of these tests, as well as bond tests of beam specimens cast without covers [32], this reduction of the bond strength is seen as too conservative. For high corrosion levels, potentially with spalling of concrete cover, it is essentially only the residual part of the local bond stress-slip relationship that provides anchorage capacity in ARC2010. This is due to the large equivalent slip for those cases. Therefore, the Regan & Reid 2009 results [32], from tests of beams without concrete covers, can serve as a reference for residual capacity where corrosion levels are high.

A modified expression of the residual bond capacity for specimens with low stirrup content is proposed for both the corroded and uncorroded cases:

$$\tau_{res,mod}(K_{tr}) = \begin{cases} (0.16 + 12K_{tr}) \cdot \tau_{bu,split,red} & for\ 0 \le K_{tr} \le 0.02 \\ 0.4 \cdot \tau_{bu,split,red} & for\ 0.02 < K_{tr} \end{cases} \quad (19)$$

The lower level was chosen to yield a residual bond capacity of 16% of the reduced splitting strength, see Equation 18. This is in the lower end of the test results mentioned above [15,30,31] and in line with Regan

& Reid's tests [32]. The upper limit, which is reached when $K_{tr}$ is greater than 0.02, was chosen based on comparison with the ARC1990 model and Regan & Reid 2009 [32].

A comparison of the residual bond stress of the previous model ARC1990, the proposed new ARC2010 model and the results of the tests by Regan & Reid 2009 are plotted for C30/37 and C50/60 concrete in Figure 7 and Figure 8, respectively. The tests denoted "flush" and "mid-barrel" have a cover of $\phi_m/2$ and zero respectively, measured from the centre of the bar.

It should firstly be noted that the dependency on concrete strength varied between the models. In ARC1990 and Regan & Reid 2009, the residual capacities are functions of the square root of the concrete strength, while in ARC2010 it is a function of the concrete strength raised to the power of ¼. This causes the latter to be less sensitive to changes in concrete strength than ARC1990 and Regan & Reid 2009.

With C30/37 concrete, shown in Figure 7, the residual capacity of ARC2010 for "Good bond conditions" is between Regan & Reid's flush and mid-barrel without stirrups, and is slightly larger for higher stirrup content. The same observation is made for ARC1990, although the capacity is greater than both ARC2010 and Regan & Reid 2009 for high stirrup content. For "All other bond conditions", ARC2010 shows results similar to those in Reagan & Reid 2009 for small stirrup levels, whilst lower capacity is shown for higher stirrup levels. Furthermore, ARC1990 shows a similar residual capacity to Regan &Reid 2009 and ARC2010 for low stirrup levels. For higher stirrup levels the residual capacity of ARC1990 is lower.

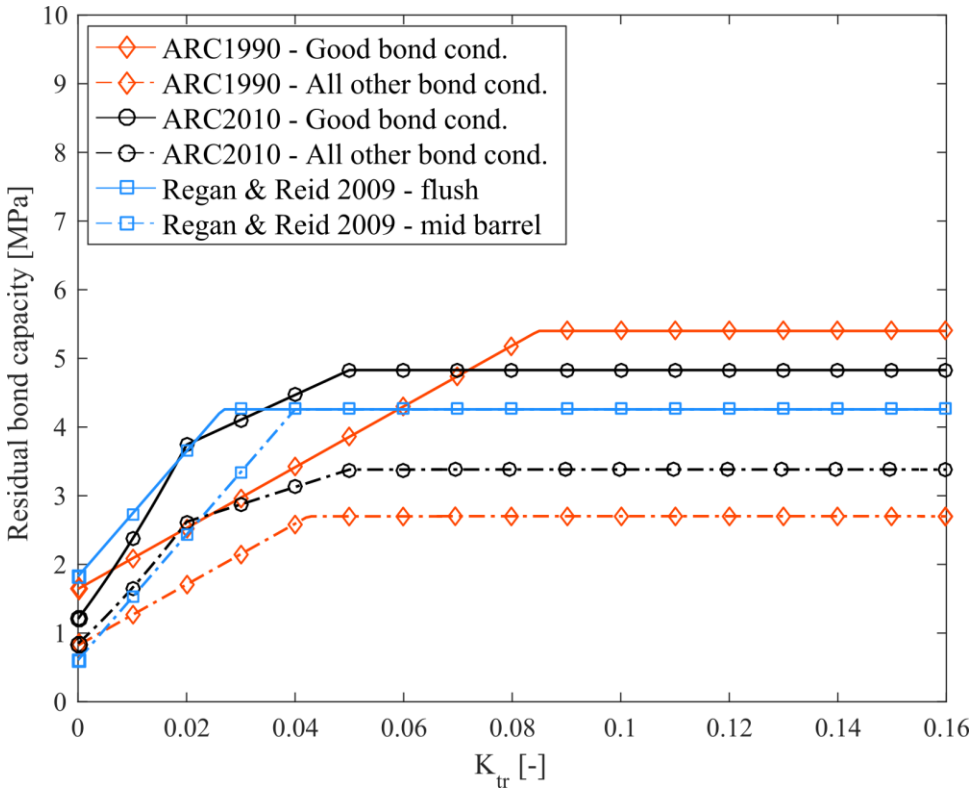


*Figure 7: Comparison of residual bond stress from ARC1990, proposed ARC2010 and results from Regan & Reid 2009 for C30/37 concrete,* $\phi_m = 20\ mm$ and $k_m = 12$.

With C50/60 concrete, depicted in Figure 8 below, the residual capacity of ARC2010 for "Good bond conditions" is in line with Regan & Reid 2009, both without stirrups and with increasing stirrup content. It can also be seen that ARC1990 corresponds well to cases without stirrups, but with increasing stirrup content it reaches a higher capacity than Regan & Reid 2009. For "All other bond conditions", ARC2010 shows similar results to Reagan & Reid 2009 for low stirrup content and a lower capacity for higher stirrup content. Furthermore, ARC1990 shows similar residual capacity as Regan & Reid 2009 for low stirrup content, but with higher stirrup content, the residual capacity of ARC1990 is lower. Overall, ARC2010 gives results that appear within an acceptable range compared to Regan & Reid 2009 and which are consistent with the physical behaviour.

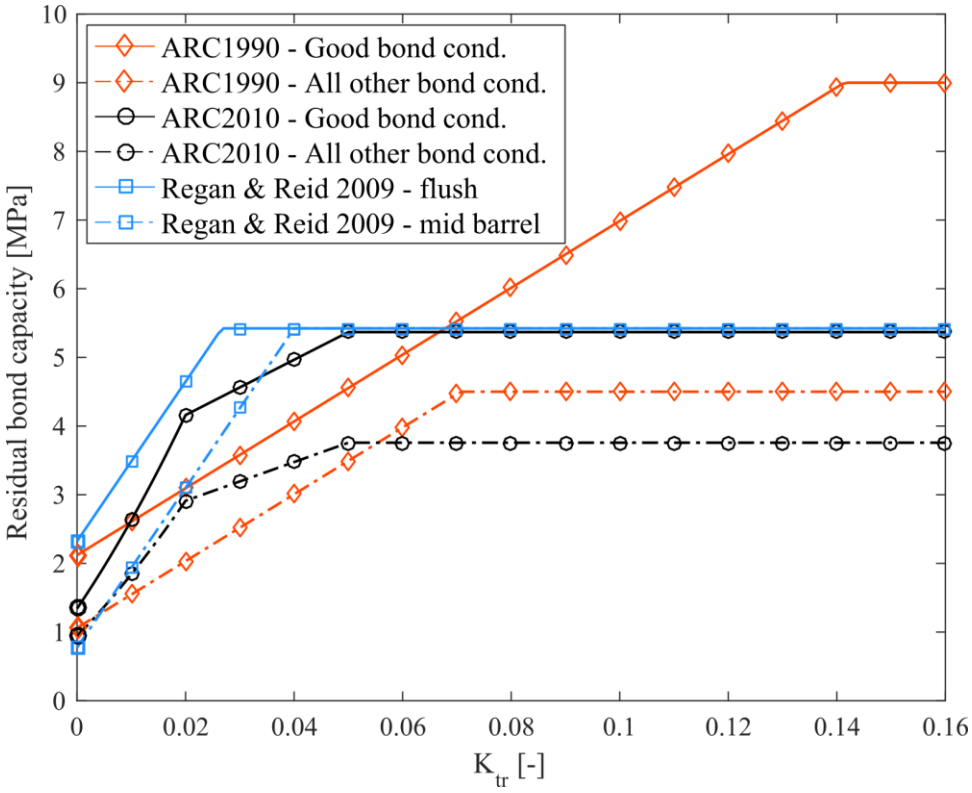


*Figure 8: Comparison of residual bond stress from ARC1990, proposed ARC2010 and results from Regan & Reid 2009 for C50/60 concrete,* $\phi_m = 20\ mm$ and $k_m = 12$.

# 3. CALIBRATION AND VERIFICATION AGAINST DATABASE

## 3.1 Description of the database

A compilation of 500 bond tests was used to calibrate the equivalent slip, which depends on the corrosion level. The database consists of pull-out and beam tests reported in 21 research works [3, 5, 6, 8, 15, 28–30, 32–44]. Information about the tests includes bar diameter $\phi_m$, concrete cover $c$, embedment length $l_b$, stirrup content $A_{st}/(s_t \cdot \phi_m)$, yielding strength of stirrups $f_{yt}$, concrete compressive strength $f_{cm}$ and the current density used in accelerated corrosion process $v$ and corrosion level $W_c$. Also included are the absolute bond strength $\tau_{DB,abs}$ (typically calculated as the anchored force divided by the surface area of the bar in the bonded zone) and the relative bond strength $\tau_{DB,rel}$, defined as the ratio between absolute bond strength of the corroded and the uncorroded (reference) test. The current densities vary among the test set-ups, which may influence the bond capacity. Moreover, the embedment lengths vary. For short embedment lengths, the absolute bond strength can be seen as the local bond strength. For longer lengths, this no longer holds true. However, the comparison between the computational model and the database results is made by assessing the anchorage capacity using a level II analysis, in other words integrating the local bond stress along the embedment length. The resulting force is then divided by the surface area of the rebar in the bonded zone to obtain the average bond strength. This also corresponds to the procedure for determining bond strength in the tests.

Many factors influence the bond strength between concrete and corroded reinforcement and bond test results are typically subjected to considerable scatter. To quantify the scatter in the database, bond test results from corroded specimens were sorted into groups based on confinement and the level of corrosion. The coefficient of variation of the relative bond strength, with respect to the uncorroded case, was then estimated within the groups. The confinement was quantified by a bond index obtained from a well-known empirical bond model, including the main parameters of confinement [45] which can be written as:

$$I_A = 0.1 + 0.25 \cdot \frac{c}{\phi_m} + 4.15 \cdot \frac{\phi_m}{l_b} + 0.024 \cdot \frac{A_{st}}{s_t \cdot \phi_m} \quad (20)$$

where $c$ is concrete cover, $\phi_m$ bar diameter, $l_b$ embedment length and $A_{st}/(s_t \cdot \phi_m)$ the amount of transverse reinforcement. The corrosion level was quantified by percentage weight loss.

Four levels were chosen for the bond index and five for the corrosion level. The inclusion intervals were selected to distribute the tests more or less evenly among the groups. The bond index groups were 0-1.0, 1.0-1.5, 1.5-2.0 and 2.0-3.0, and the corrosion level groups were 0-1.5%, 1.5-3.0%, 3.0-4.5%, 4.5-10% and 10-%. Uncorroded cases were filtered out. Thus, a total of 460 bond test results were divided into 20 (4x5) groups. The distribution of the tests among the groups is presented in Figure 9.

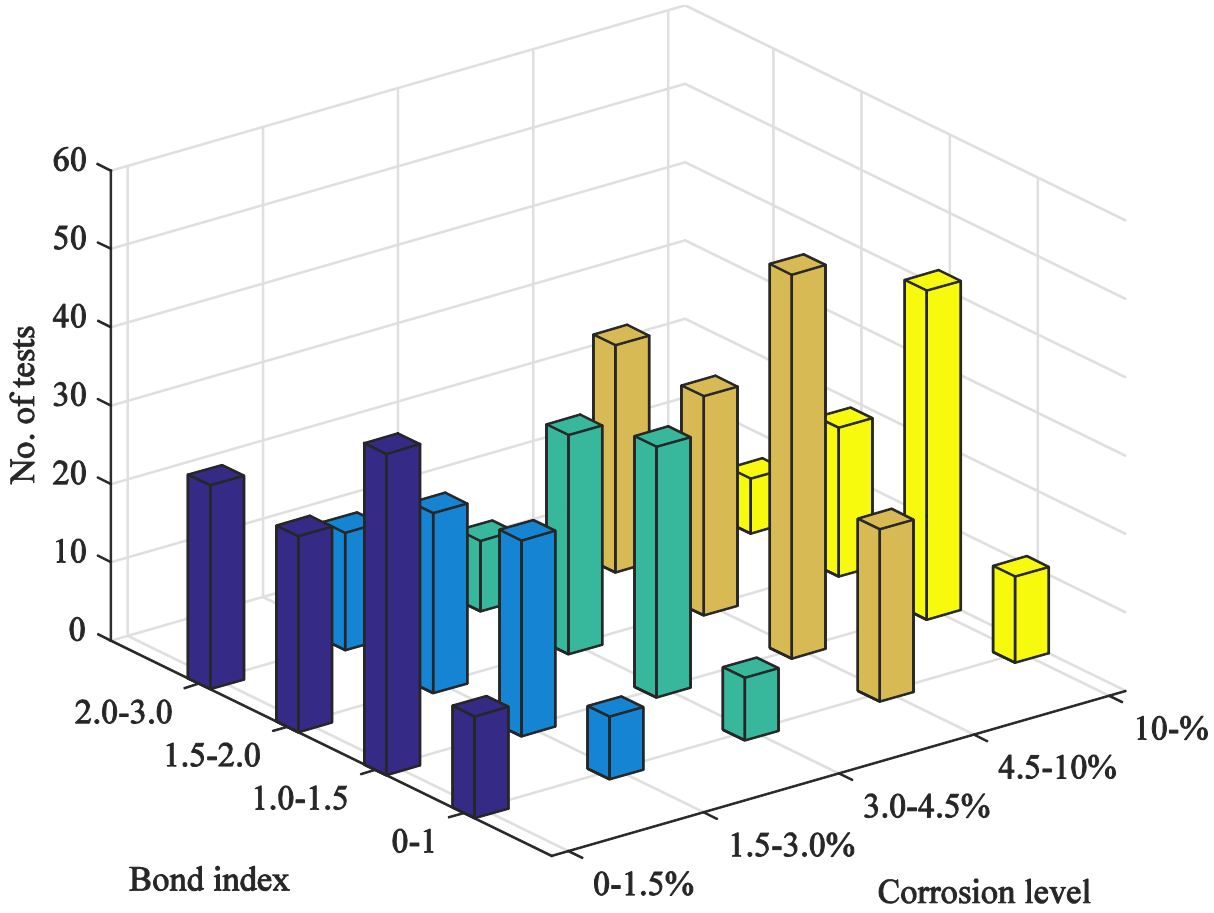


*Figure 9: The four bond index intervals and the five corrosion level intervals are presented on the horizontal axes. The number of test results in each group is presented on the vertical axes.*

Incidentally, the maximum levels of corrosion applied in tests are often related to the experimental time needed, as high corrosion levels also should be reached with a sufficiently slow corrosion speed. Furthermore, for low levels of corrosion the variation in weight of a steel bar from the production of the reinforcement can be important. For example, if a specific bar is not weighed before corrosion is applied (as is common in experimental works) but instead nominal values are used.

Within each of the 20 groups, the relative bond strength was used to estimate the coefficient of variation. It was calculated as the standard deviation divided by the mean value of the relative bond strengths in the groups, see Equations 21-23:

$$c_v = \frac{\sigma}{\mu} \tag{21}$$

$$\sigma = \sqrt{\frac{1}{N-1}\sum_{i=1}^{N}\left|\tau_{DB,rel,i} - \mu\right|^2} \tag{22}$$

$$\mu = \frac{1}{N}\sum_{i=1}^{N}\tau_{DB,rel,i} \tag{23}$$

where $N$ is the total number of tests in the group and $\tau_{DB,rel,i}$ is the relative bond strength in test $i$.

A contour plot of the coefficient of variation appears in Figure 10. This shows that the highest coefficient of variation is associated with the group having a bond index of 2.0-3.0 and a corrosion level between 4.5-10%. If the confinement stems from a large concrete cover with only a minor contribution from stirrups, the bond strength can be expected to decrease suddenly once the cover is cracked by corrosion. If instead the confinement is mostly provided by stirrups, then a larger remaining capacity can be expected after corrosion-induced cracking. Therefore, the variation in this group is reasonable. The coefficient of variation is lower along the left and bottom boundaries of the contour plot, i.e. either low bond index (0-1.0) or low corrosion level (0-1.5%). This is because corrosion cracking has less impact on bond in these cases; for specimens with low bond index because they are likely to crack due to mechanical loading only, and for low corrosion levels as the cover is likely not cracked by corrosion. This explains why the coefficient of variation is smaller along the left and bottom boundaries.

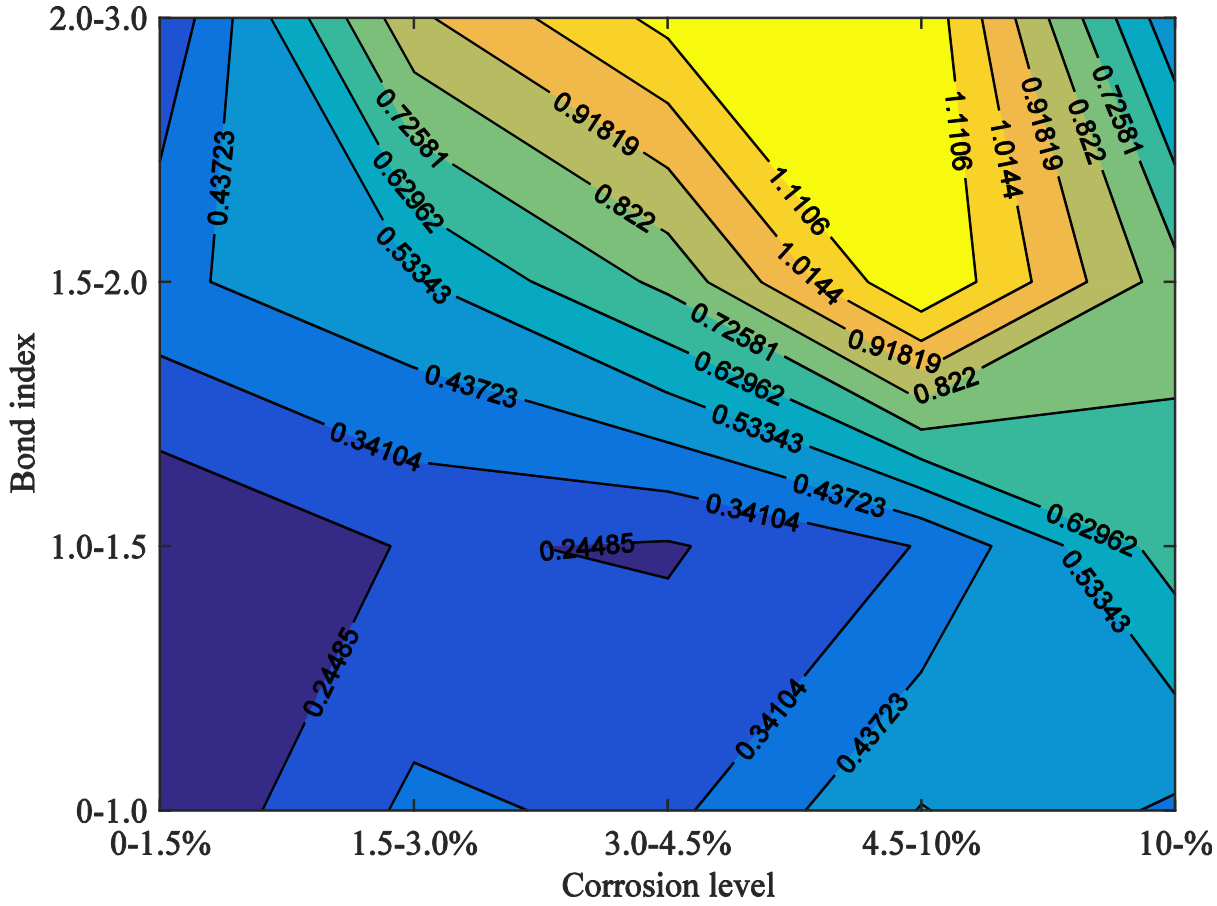


*Figure 10: Contour plot of the coefficient of variation for relative bond strength in the database of varying bond index and corrosion level.*

Coefficients of variation of up to 110% illustrate major experimental scatter, as is common for bond test results of corroded reinforcement in concrete. This should be borne in mind when validating the ARC2010 model in Section 3.3.

## 3.2 Determination of the equivalent slip

The bond test results from the database described above were used to find the equivalent slips for ARC2010, by solving the inverse problem according to the concept described in Section 2.3.1. Using the equivalent slips, the assessment model should give relative bond strengths corresponding to the test results in the database. However, due to scatter in the test results and since increased bond capacity due to low levels of corrosion is not included in ARC2010, the comparison between model and test results should be made carefully.

Moreover, to obtain a sound basis for the calibration two exclusion criteria were applied to the tests in the database. The maximum allowable current density for inclusion in the calibration was 400 $\mu A/cm^2$. Higher current densities have been shown to influence the steel concrete bond extensively, see for example [46]. This excluded 180 tests from the calibration data. Furthermore, some test results were excluded from the calibration as their bond capacity was deemed unreasonably high. Such results may be due to the difference between intended and actual embedment length or influence of transverse pressure. The choice of which tests to exclude was made by limiting the maximum bond stress to the maximum shear stress as per Mohr-Coulomb failure criterion, without considering adhesion. By setting the third principal stress as the compressive capacity and the first principal stress as zero, the maximum bond stress may be written:

$$\tau_{DB,abs} \leq \frac{f_{cm}}{2} \tag{24}$$

For the presence of stirrups, a choice was made to increase the limit on the maximum bond stress by 20% due to additional confinement. This was because compressive stresses surrounding corroding main bars can arise where stirrups hold the cross section together, due to the volume increase of the main bars. These compressive stresses in the surrounding concrete can lead to additional bond capacity. The value of 20% was chosen based on the provisions for additional capacity due to transverse pressure in Model Code 2010 [23]. This criterion excluded an additional 43 tests and the remaining 277 tests were included in the calibration.

### 3.2.1 Equivalent slip from the normalised average bond strength in the database

The equivalent slip in the model was calibrated to produce the same average bond strength for the ARC2010 model as in the tests, both normalised with respect to the uncorroded cases. Firstly, the reference average bond strength was calculated using ARC2010 without applying corrosion. Then an equivalent slip was found for each test, yielding the corresponding reduction of normalised average bond strength as in the database. If the corrosion level was high enough to crack the concrete cover, the local bond stress-slip relationship was changed according to Section 2.3.2, prior to finding the equivalent slip. This inverse problem was solved in an iterative procedure.

For two types of cases it was not possible to achieve the same normalised average bond strength as in the database:

- Corrosion caused increased average bond strength in the test. The equivalent slip for ARC2010 was set to zero, i.e. yielding no reduction in bond strength.
- The normalised average bond strength in the test was less than the normalised residual bond strength in ARC2010. The smallest equivalent slip yielding the normalised residual bond strength

of ARC2010 was selected. If a larger equivalent slip value was chosen, this might lead to an overly conservative model.

Moreover, in test specimens without stirrups, the peak of the bond stress curve can be narrow, which in some cases caused convergence problems in the iterative procedure above. For those cases, an equivalent slip was found manually by selecting a value that gave as close a reduction as possible to the test results.

### 3.2.2 Calibration of equivalent slip function

The different input parameters for the ARC2010 model listed in Table 3 were complemented with the corrosion level. The influence on the equivalent slip of all these parameters were investigated by plotting the equivalent slip against each input parameter one at a time. The only parameter showing a clear relationship was the corrosion level; as expected the equivalent slip increases with corrosion level.

The database was split into two groups due to the different bond stress-slip relationships between cases with and without stirrups. One group included the test specimens with stirrups, and the other without. Furthermore, each group was randomly divided into two sets, approximately 80% of the data were put in a set used for calibration and the remaining 20% in a verification set. The size of the calibration and verification set was determined on the basis that the calibrated models for the equivalent slip should perform equally well, as measured by the mean squared error, on the calibration and verification set, in order to not over-fit the data.

Two different functions for the equivalent slip were calibrated, one for cases with stirrups and one for cases without. The linear regression was carried out using MATLAB [47] (commercial software) by determining the least squares fit. The linear function was prescribed to pass through the origin, to prevent a sudden increase in equivalent slip at very low corrosion levels.

The functions yielding the best fit were thus determined, as shown in Equations 25 and 26, for cases without and with stirrups respectively:

$$s_{eq,nostir} = 2.9W_c \qquad \text{without stirrups} \qquad (25)$$

$$s_{eq,stir} = 13.6W_c \qquad \text{with stirrups} \qquad (26)$$

where $W_c$ is the corrosion level (weight loss) in decimals and the equivalent slip is output in mm. For cases without stirrups there is data up to around 15% corrosion, and for cases with stirrups up to approximately 20% corrosion. Therefore, the domains for Equation 25 and 26 are 0-15% and 0-20% corrosion weight loss, respectively.

The expressions for the equivalent slips are plotted in Figure 11. This shows that the equivalent slip for cases with stirrups is markedly higher than in cases without stirrups. This is reasonable, keeping in mind that it is the change in resulting average bond stress from a level II analysis that is fitted. Moreover, the local bond stress-slip relationships for cases without transverse reinforcement show a steep reduction after the maximum bond strength value, whereas the reduction for cases with transverse reinforcement is less. In other words, a smaller shift in the local bond stress-slip curve is required for the non-stirrup cases to yield a similar reduction in relative bond strengths to the stirrup cases. The equivalent slip for the previous model, ARC1990, is computed as the corrosion penetration multiplied by the constant 8.1 [18,19], a value

obtained from a parameter study using FE analyses. The equivalent slip for $\phi_m = 10\,mm$ and $\phi_m = 25\,mm$ reinforcement bars are also included in Figure 11. It would be overly conservative to use this expression for the ARC2010 model, especially for cases without stirrups.

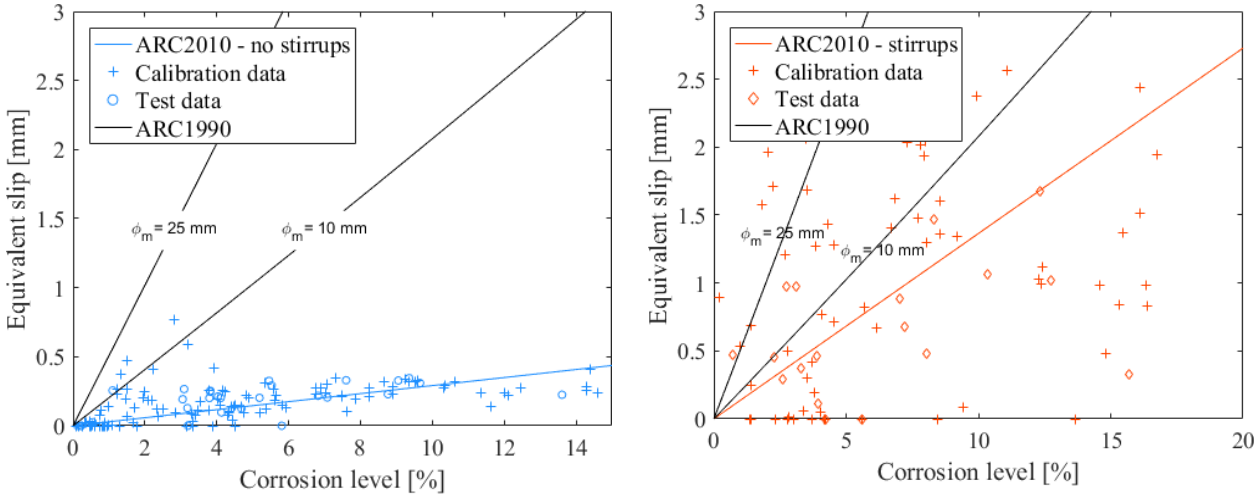


*(a) Cases without stirrups* *(b) Cases with stirrups*

*Figure 11: Presentations of the expressions of equivalent slips for ARC2010 and ARC1990, plus calibration and verification data.*

## 3.3 Verification of the proposed model

As just described, the database was used to find equivalent slips for ARC2010 which yielded similar reductions in average bond strength by inverse analysis, i.e. finding the input that yields the desired output. These equivalent slips were then used to calibrate linear functions, see Equations 25 and 26. ARC2010 was run against all the bond tests in the database using the equivalent slips determined by the expressions, so as to demonstrate the applicability of the proposed model. This included changes in the local bond stress-slip relationship due to cover cracking from corrosion and modification of residual strength as per Sections 2.3.2 and 2.3.3 respectively. The resulting normalised average bond strengths from ARC2010 were also compared to an empirical model by Castel *et al.* [48] and experimental bond stress-slip relationships.

### 3.3.1 Comparison to database results

The relative average bond strengths obtained from the ARC2010 model, i.e. the deteriorated bond strength normalised by the non-corroded bond strength, are plotted against the corresponding database values for cases without and with stirrups in Figure 12. Intentionally, no increase in relative bond strength is allowed for ARC2010, however a number of tests in the database show increased capacity. As stated earlier, the scatter among the bond test results is quite large which can be seen in the plots. However, it may also be noted that the results are equally distributed around the diagonal line, representing same result in database and ARC2010, however with a slight skew towards the safe side.

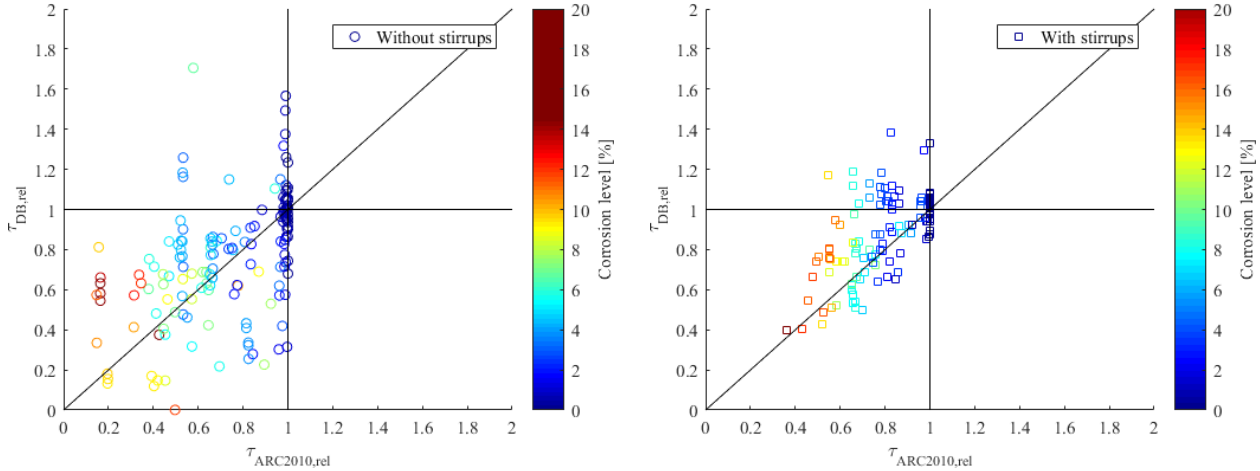


*(a) cases without stirrups* *(b) cases with stirrups*

*Figure 12: Normalised average bond strength from database versus ARC2010 model for specimens without stirrups (a) and specimens with stirrups (b). The diagonal line corresponds to full agreement.*

The absolute average bond strengths obtained from the ARC2010 model are plotted against the corresponding database values for cases without and with stirrups in Figure 13. It is observed that for cases with stirrups, the ARC2010 model more often predicts higher average bond strengths compared to the test results. This is most pronounced for the uncorroded cases, for which the original Model Code 2010 is used, while the agreement gets better with increased corrosion.

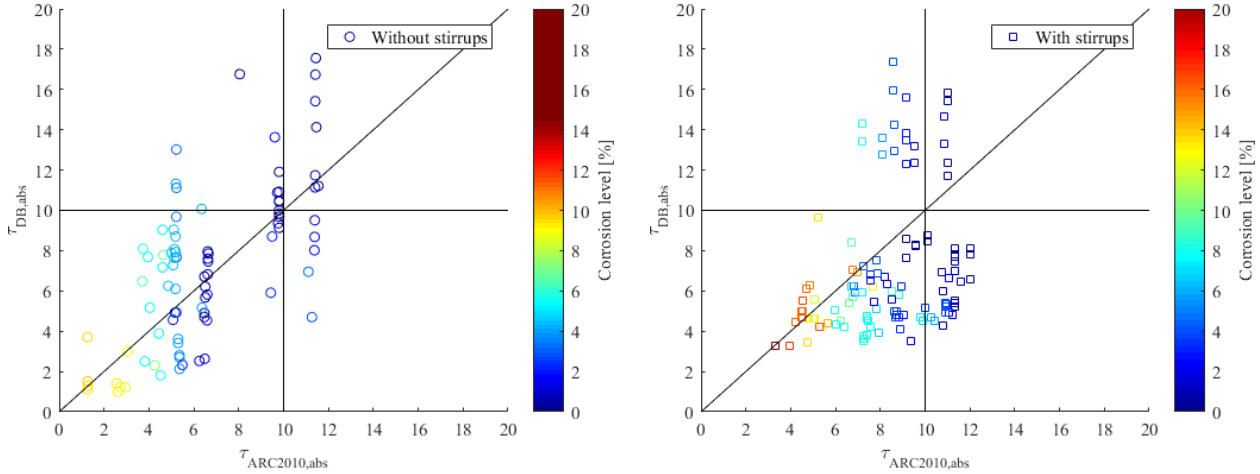


*(a) cases without stirrups* *(b) cases with stirrups*

*Figure 13: Absolute average bond strength from database versus ARC2010 model for specimens without stirrups (a) and specimens with stirrups (b). The diagonal line corresponds to full agreement.*

Since the scatter of the database is rather large, traditional measures of goodness of fit such as the $R^2$ value can be misleading. Here, the residuals obtained when subtracting the ARC2010 results from the database results are studied instead ($\tau_{DB,rel} - \tau_{ARC2010,rel}$). The residuals for the cases without stirrups are presented in Figure 14. No obvious bias is visible to any side of the horizontal line due to the corrosion level. The mean value of the residuals (sign included), is 0.05 for the cases without stirrups.

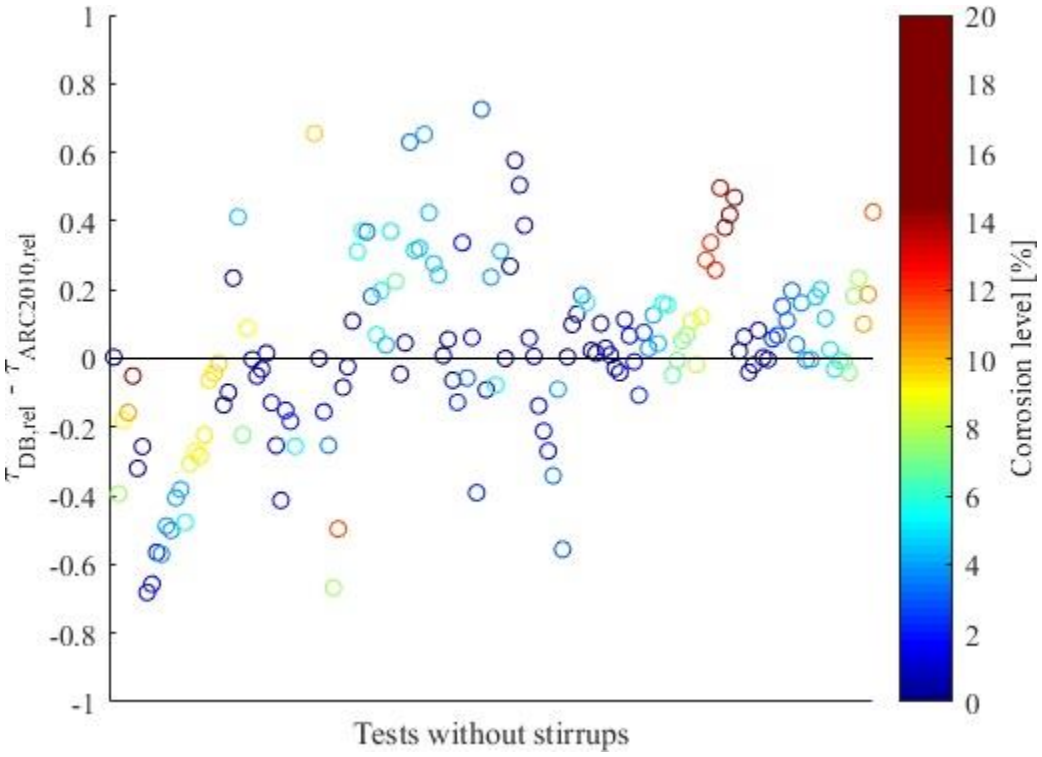


*Figure 14: Residual between normalised average bond strength in database and ARC2010 for cases without transverse reinforcement. Positive values mean larger database capacity.*

The residuals for cases with stirrups are plotted in Figure 15. The mean value of the residuals (sign included) is 0.09 for the cases with stirrups.

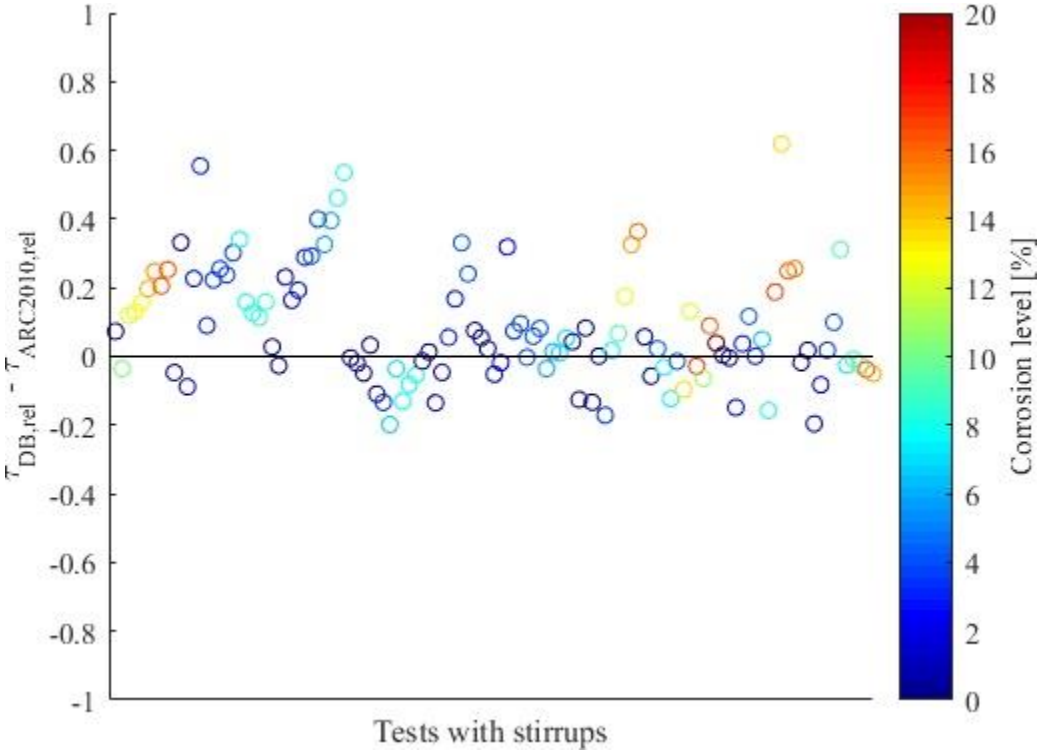


*Figure 15: Residual between normalised average bond strength for database and ARC2010 for cases with stirrups. Positive values mean larger database capacity.*

### 3.3.2 Comparison to empirical model by Castel *et al.* 2016

The ARC2010 model was compared to the empirical model by Castel *et al.* 2016 [48] in terms of relative bond strength for several corrosion levels. The applicability of the Castel *et al.* 2016 model was verified against a large data set (partially coincident with data used for ARC2010 calibration) and compared with good agreement to several other empirical expressions. Other models of the bond strength of corroded reinforcement were also considered, such as Prieto *et. al.* 2016 [49]. The Castel *et al.* 2016 model was chosen because the corrosion is quantified by the area of cross-section loss. This was deemed interesting in the comparison to ARC2010 as it is based on corrosion as a percentage. For a complete description of the empirical model please refer to [48].

Figure 16 presents a comparison for the case with $f_{ck} = 50\ MPa$, $\phi_m = 16$ mm, without stirrups and for three different concrete covers ($c = 40, 60$ and $80$ mm). As can be seen, the relative bond strengths obtained from the two models agree well. For the ARC2010 model, three main corrosion intervals can be identified. For low levels of corrosion, the concrete cover is not yet cracked. Cracking of the cover leads to a marked decrease in relative bond strength. This occurs at around 2% corrosion level for $c = 40$ mm, 3% for $c = 60$ mm and 5% for $c = 80$ mm. Within the next corrosion level interval, the reduction springs solely from application of the equivalent slip. This continues until the equivalent slip being applied is sufficiently large to leave only the residual capacity in the local bond stress-slip curve. This corresponds to the last corrosion interval.

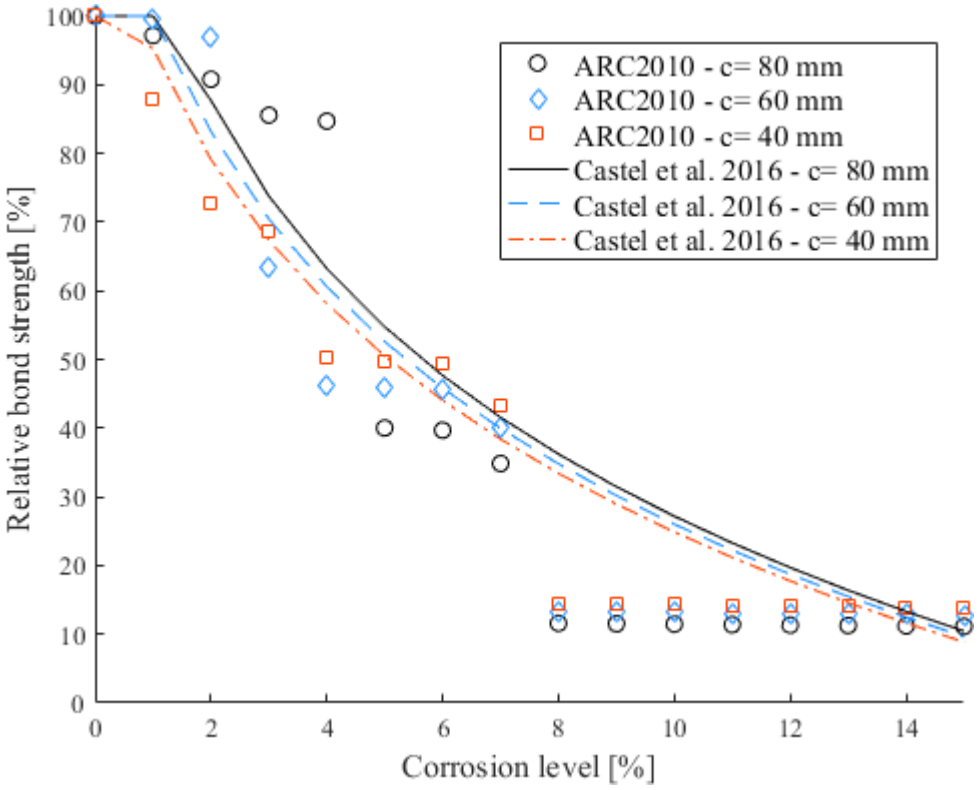


*Figure 16: Comparison between Castel et al. 2016 and ARC2010 for $f_{ck} = 50\ MPa$, $\phi_m = 16\ mm$, without stirrups.*

A similar case is compared in Figure 17, but differing by the stirrup content of $\phi_t = 8$ mm with spacing $s_t = 150$ mm. The reduction in relative bond strength is pronounced for cases with stirrups when corrosion causes cracking of the concrete cover. Thereafter, the bond capacity decreases as the corrosion level increases but without the sudden drop in residual capacity. This case also shows a good agreement between Castel *et al.* 2016 and ARC2010, although the latter yields a higher capacity for higher levels of corrosion.

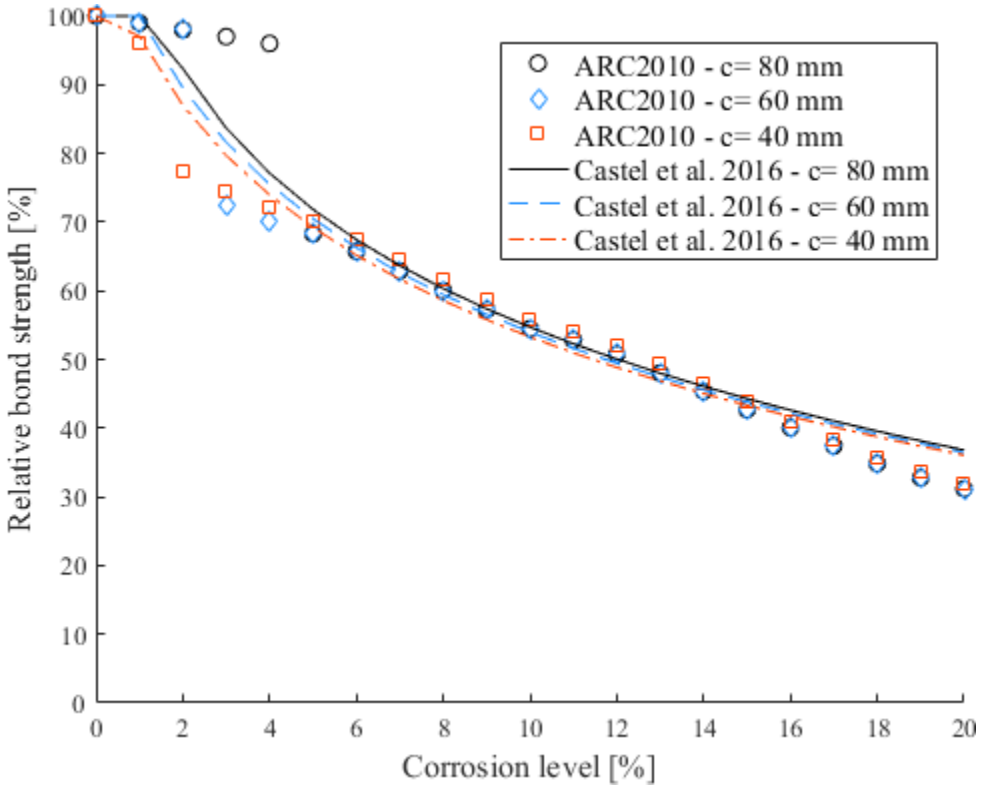


*Figure 17: Comparison between Castel et al. 2016 and ARC2010 for* $f_{ck} = 50\ MPa$, $\phi_m = 16\ mm$, $\phi_t = 8\ mm$ *and* $s_t = 150\ mm$.

The case with the similar stirrup diameter but half the stirrup spacing ($\phi_t = 8$ mm with spacing $s_t = 150$ mm) is presented in Figure 18. The results are analogous to those in Figure 17, while the drop in capacity at concrete cover cracking is less pronounced due to the larger amount of stirrups. This can be explained by much of the capacity originating from the transverse reinforcement, occasioning less influence by the concrete cover.

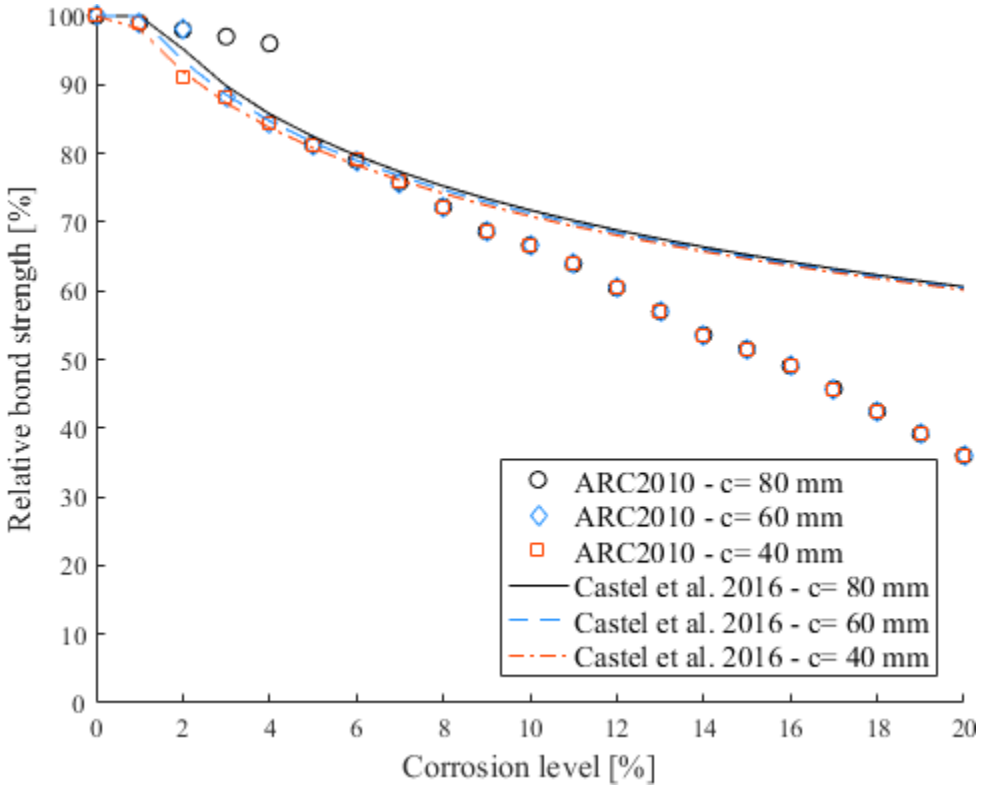


*Figure 18: Comparison between Castel et al. 2016 and ARC2010 for $f_{ck} = 50\ MPa$, $\phi_m = 16\ mm$, $\phi_t = 8\ mm$ and $s_t = 75\ mm$.*

### 3.3.3 Comparison to experimental bond stress-slip relations

In this section, the local bond stress-slip relationships obtained from the ARC2010 model are compared with relationships obtained from experiments. The pull-out tests with plain concrete performed by Berrocal *et al.* 2017 [50] serves as comparison for cases without stirrups. Geometrical data of the test specimens and the input parameters for the ARC2010 model are presented in Table 4. As the embedment length in the tests was shorter than five times the diameter, a constant bond stress along the embedment length was assumed when the local bond stress from the tests was calculated.

*Table 4: Geometrical data for pull-out test specimens from Berrocal et al. 2017 and model parameters used in ARC2010 model.*

| **Parameter** | **Value** |
|---|---|
| Embedment length [mm] | 70 |
| Main bar diameter $\phi_m$ [mm] | 16 |
| Cover x-dir $c_x$ [mm] | 64 |
| Cover y-dir $c_y$ [mm] | 64 |
| Concrete compressive strength $f_{cm}$ [MPa] | 56 |
| Young's modulus $E_s$ [GPa] | 200 |
| Yield strength main bars $f_y$ [MPa] | 500 |
| Alpha factor $\alpha$ [-] | 0.4 |
| $c_{clear}$ [mm] | 6.5 |

| | |
|---|---|
| Bond conditions $\eta_2$ [mm] | 1 |

The results from the pull-out tests together with the results obtained from the ARC2010 model are presented for uncorroded and moderate levels of corrosion in Figure 19. Note that the average corrosion level of the three tests is used as input for the ARC2010 model. It can be seen that the maximum local bond stress agrees reasonably well between the experiments and the model, especially for the case with corrosion. The residual branch of the local bond stress-slip curve is however overestimated by the model. This is expected since very limited confinement if present after the concrete cover of the circular pull-out test specimens are cracked. The ARC2010 is however adjusted to have a residual bond stress as is common in more real situations such as bars in beams or slabs, as described in Section 2.3.3.

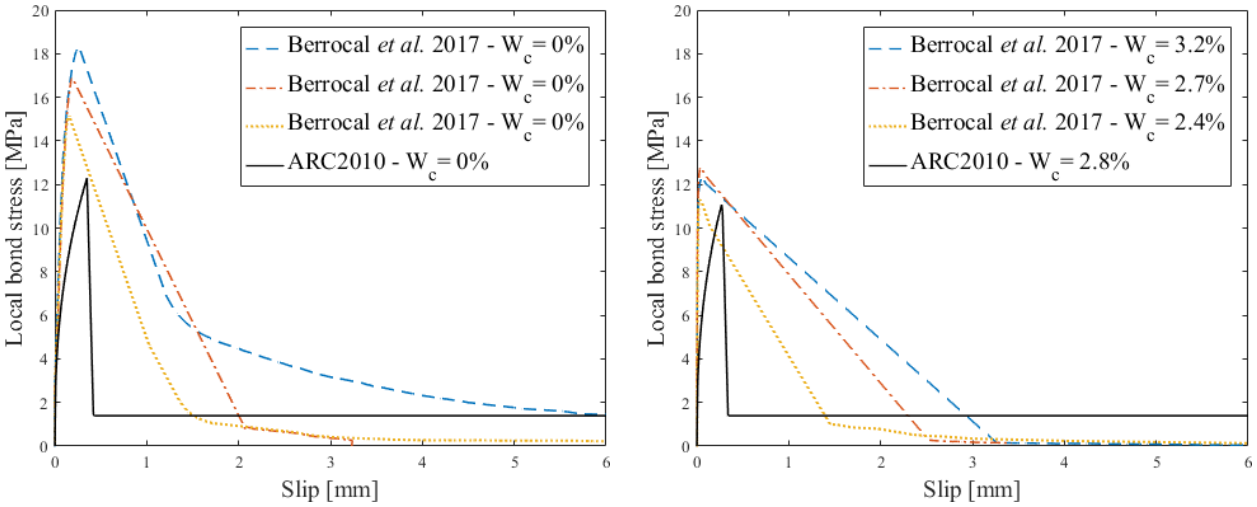


*(a) uncorroded* *(b) moderate corrosion level*

*Figure 19: Comparison between ARC2010 and experiments without stirrups.*

Furthermore, beam tests including transverse reinforcement from Lin and Zhao 2016 [29] were used for comparison. The beams had stirrups with spacing of both 100 mm and 150 mm. The geometrical and model input parameters are given in Table 5. As the embedment length in these tests were longer than five times the diameter, the average bond stress from experiments and the ARC2010 model were compared for varying levels of corrosion, see results in Figs 20-21. As can be seen, the model is able to represent the average bonds stress-slip relationships rather well, both in terms of the peak bond stress as well as the residual bond strength. For the uncorroded cases the ARC2010 model, that is the original Model Code 2010, is shown to overestimate the peak bond stress slightly. With increasing corrosion level this overestimation becomes smaller.

*Table 5: Geometrical data for beam test specimens and model parameters used in ARC2010 model.*

| **Parameter** | **Value** |
|---|---|
| Embedment length [mm] | 150 |
| Main bar diameter $\phi_m$ [mm] | 20 |
| Cover x-dir $c_x$ [mm] | 40 |
| Cover y-dir $c_y$ [mm] | 65 |
| Concrete compressive strength $f_{cm}$ [MPa] | 30 |
| Young's modulus $E_s$ [GPa] | 200 |

| | |
|---|---|
| Yield strength main bars $f_y$ [MPa] | 540 |
| Stirrup diameter $\phi_s$ [mm] | 6 |
| c-c stirrups $s_t$ [mm] | 100/150 |
| Efficiency of stirrups $k_m$ | 12 |
| Alpha factor $\alpha$ [-] | 0.4 |
| $c_{clear}$ [mm] | $0.39\phi_m$ |
| Bond conditions $\eta_2$ [mm] | 1 |

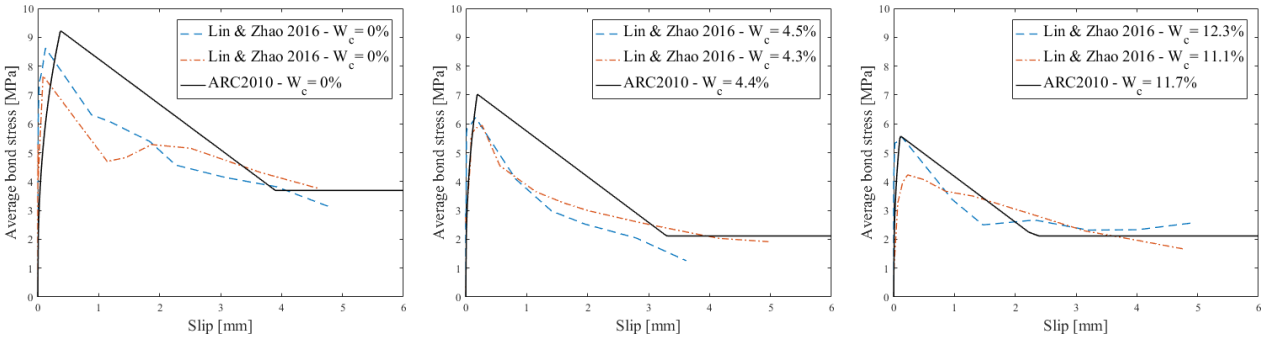


*(a) uncorroded* *(b) moderate corrosion level* *(c) high corrosion level*

*Figure 20: Comparison between ARC2010 and experimental results for cases with 150 mm stirrup spacing.*

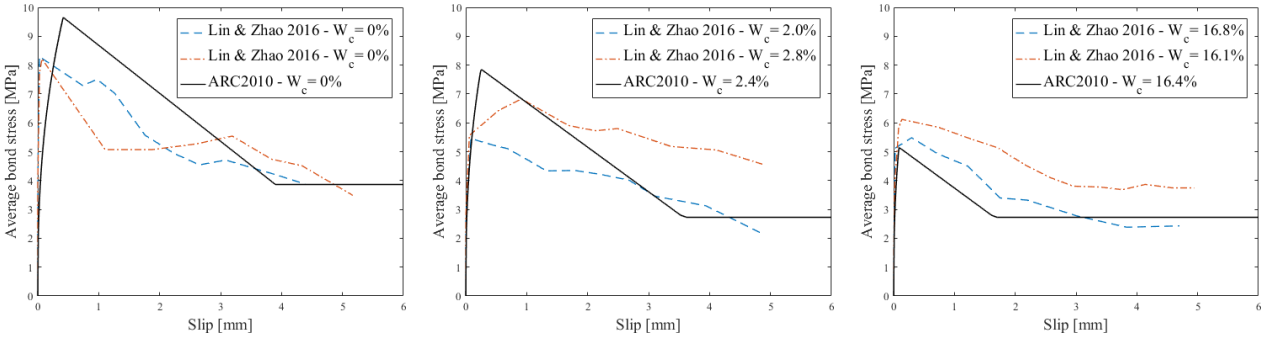


*(a) uncorroded* *(b) moderate corrosion level* *(c) high corrosion level*

*Figure 21: Comparison between ARC2010 and experimental results for cases with 100 mm stirrup spacing.*

# 4. DISCUSSION

## 4.1 Influence of scatter in the database

Many parameters influence the bond between reinforcement and concrete; even more so in the case of corrosion. Due to the large number of influencing parameters, many of which are difficult to control in experiments, the scatter in bond test results involving corroded reinforcement is expected to be large. This was also confirmed in the description of the bond database in Section 3.1.

Despite the large degree of scatter, ARC2010 can predict the reduction in bond capacity for the experiments in the database reasonably well. This claim is based on the study of residuals between the bond reduction predicted by ARC2010 and the bond tests. These have a mean value close to zero, with or

without stirrups. The possibility of reducing scatter was investigated by including more parameters in the expressions for equivalent slip. However, no significant reduction in scatter of the relative average bond strength was achieved by including parameters other than the corrosion level.

### 4.2 Use of corrosion level compared to use of corrosion penetration or area loss

There is no consensus in the research community what measure of corrosion to use, both absolute measures such as area loss in $mm^2$ and dimensionless measures such as the corrosion level as a percentage are used. The latter is used in the present model; this choice is elaborated in this section by considering three ways of quantifying the degree of corrosion: corrosion level as a percentage, penetration in mm, and area loss in $mm^2$.

The corrosion level as a percentage includes the bar diameter in the sense that the corroded portion of the cross section is given, but not in the amount of corrosion products formed since the original bar size is not included. Tests typically measure the percentage weight loss. Corrosion penetration, on the other hand, does not directly account for the bar diameter. For example, a corrosion penetration of $100\ \mu m$ means a greater reduction of a small-diameter bar than in a large-diameter bar. Several researchers therefore use the dimensionless ratio between corrosion penetration and bar radius, which is proportional to the weight loss as a percentage. The area loss due to corrosion accounts for the cross-sectional area lost to corrosion, but not how it relates to the uncorroded cross-section. For example, a highly corroded small-diameter bar might have the same area loss as a larger-diameter bar with less corrosion.

Giving corrosion as corrosion level or area loss provides no information about the distribution along or around the reinforcement. However, this potentially important information can be included by using corrosion penetration. The corrosion distribution around or along the bar was rarely specified for the tests in the database. Rather, the corrosion was described using reinforcement bar weight loss and surface crack width. Furthermore, in previous investigations by one of the co-authors of this paper [21], four corrosion distributions were studied using a 3D NLFE analysis. Corrosion was applied to: all, three-quarters, half and one-quarter of the surface area of the reinforcement bar. All cases were subjected to the same corrosion weight loss. The results showed that the relative bond strength and crack pattern were influenced only marginally by the distribution. This can be explained by the force equilibrium between the reinforcement bar and surrounding concrete, which is nearly independent of the pressure distribution around the bar.

A key question for the choice of corrosion measure for the ARC2010 model was the suitability for calibrating an expression to the equivalent slips. Therefore, the equivalent slips were plotted against the three measures of corrosion, see Figure 22 and Figure 23 for tests without and with stirrups respectively. Tests with a corrosion level below 20% are included in the plots and the calibrated expressions of the equivalent slip in ARC2010.

The tests without stirrups show that when the equivalent slips are plotted against the corrosion level, the scatter has an increasing trend but there is no clear influence from bar diameter. However, when the equivalent slips are plotted against the corrosion penetration instead, it is apparent that the greater bar diameters are shifted to the right. This indicates that greater corrosion penetration is present for bars of greater diameter. The same observation can be made when corrosion is expressed as area loss, but the shift to the right is even more pronounced for greater-diameter bars.

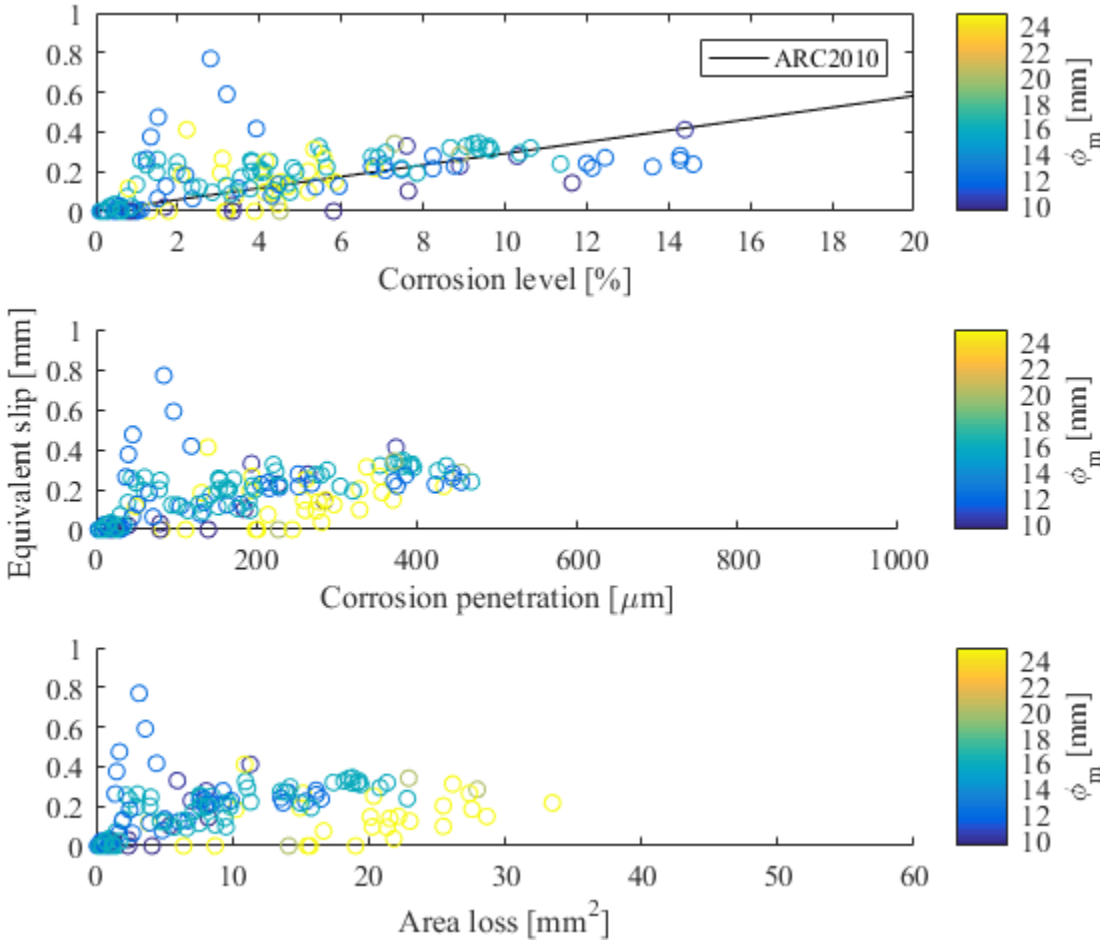


*Figure 22: Equivalent slips versus corrosion level, corrosion penetration and cross-sectional loss for cases without stirrups.*

The scatter in the equivalent slips for cases with stirrups is large and it is hardly possible to draw any conclusion about corrosion measurement and bar diameter. However, it is notable that when corrosion level is used, the different bar diameters are more evenly distributed along the corrosion scale whilst for corrosion penetration and area loss, smaller bar diameters are clustered on the left-hand side.

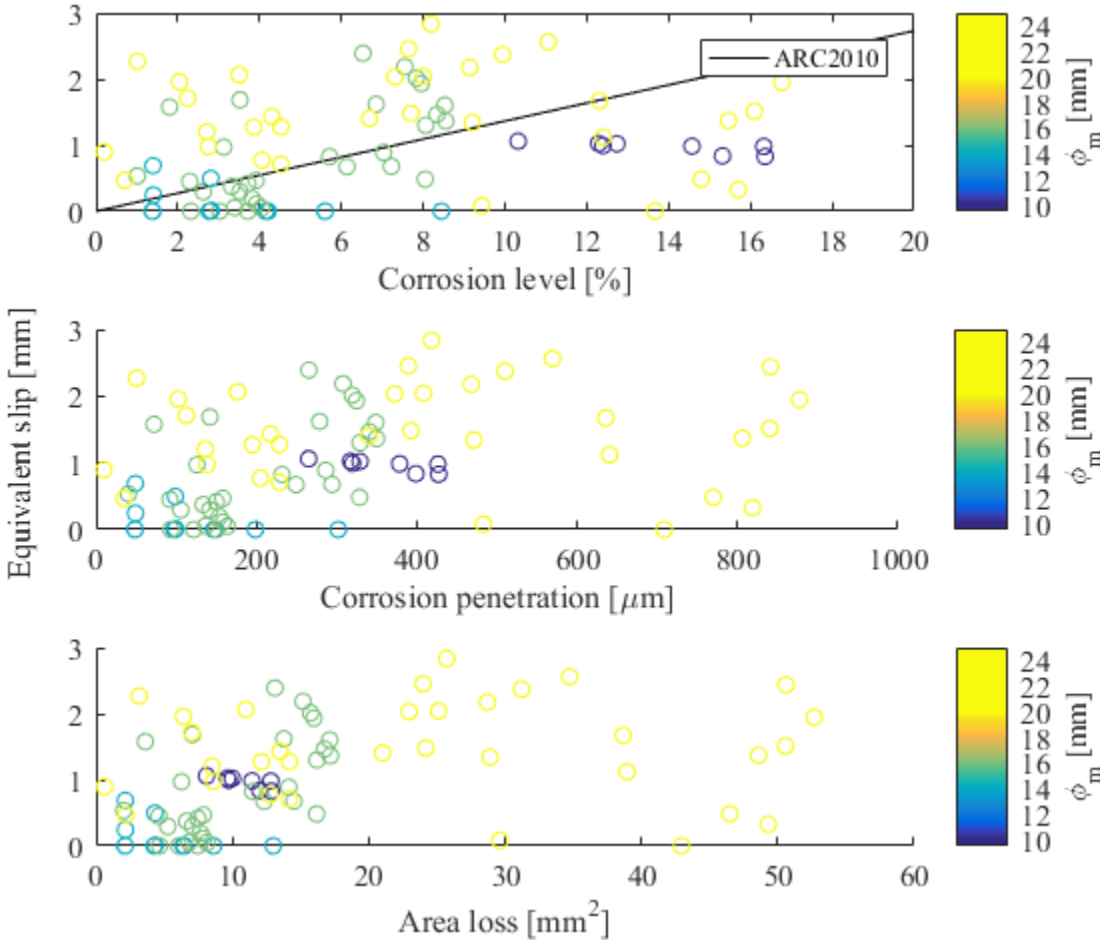


*Figure 23: Equivalent slips versus corrosion level, corrosion penetration and cross-sectional loss for cases without stirrups.*

It should be mentioned that like the model proposed by Castel *et al.* 2016, the ARC2010 model gives a greater reduction in relative bond capacity for larger bars, at a given percentage of corrosion. This is because the expression for splitting strength depends on bar diameter and greater diameter gives lower strength. Since the splitting strength and therefore also the slip values $s_1$,$s_2$ and $s_3$ (if no stirrups) decrease with increased bar diameter, the same equivalent slip gives a greater reduction in average bond strength.

Based on the plots, no definitive conclusion regarding the best general measure for corrosion can be drawn. However, corrosion level as a percentage was deemed the best option for the ARC2010 model. This was due to the independence of the bar diameter and the slightly clearer trend between equivalent slip and corrosion.

### 4.3 Comparison between ARC2010, ARC1990 and Castel *et al.* 2016

The previous ARC1990 model was applied and the results compared to the database values. The applied equivalent slip shows a linear increase with the corrosion level, as indicated in Figure 11. Figure 24 shows the results for cases without stirrups. This shows that in many cases ARC1990 predicts larger reductions in the average bond capacity compared to database values. These values are clustered on the left-hand side in the figure.

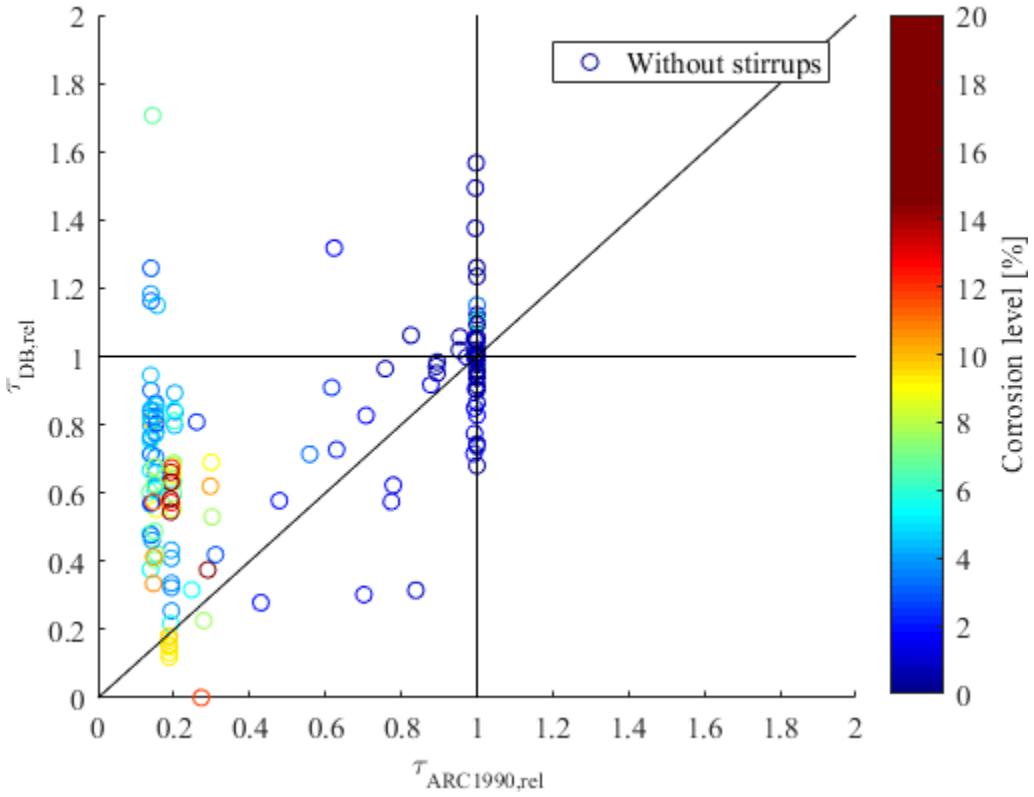


*Figure 24: Normalised average bond strength from database versus ARC1990 model for specimens without stirrups. The diagonal line corresponds to full agreement.*

Figure 25 shows the results for cases with stirrups, which appear less clustered compared to those without stirrups. However, the ARC1990 model shows a trend towards greater reduction in average bond capacity compared to database values for cases with stirrups.

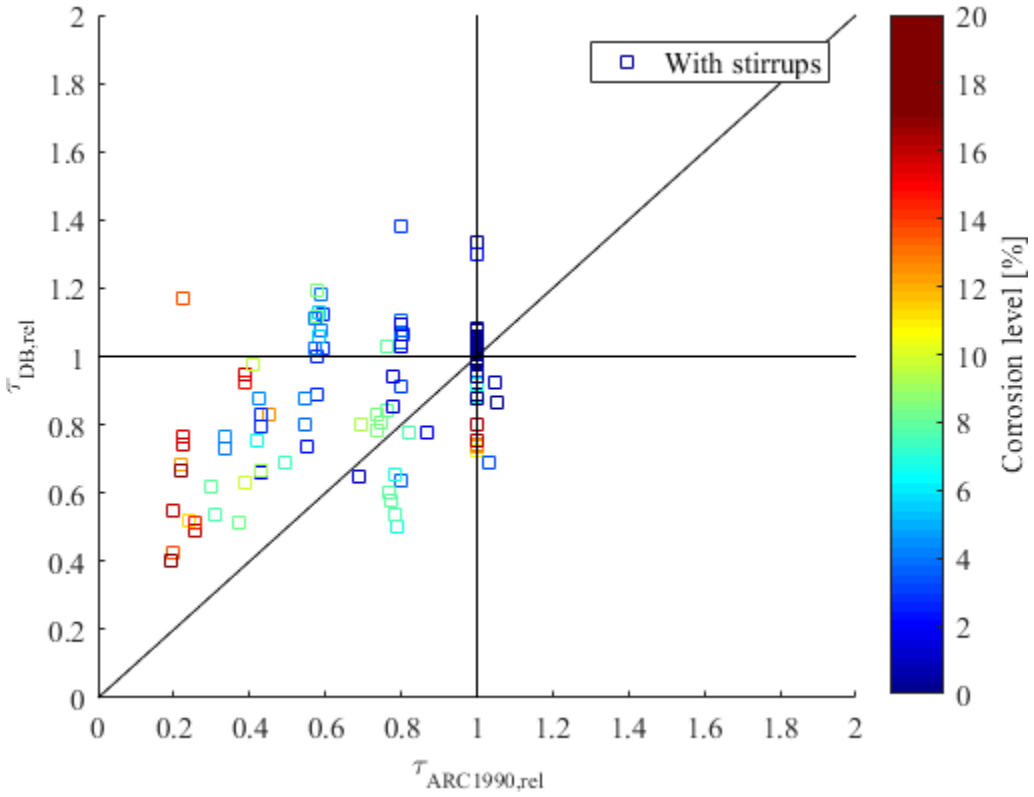


*Figure 25: Normalised average bond strength from database versus ARC1990 model for specimens with stirrups. The diagonal line corresponds to full agreement.*

ARC2010, ARC1990 and the empirical expression given by Castel et al. 2016 [48] are compared in Table 6. This is achieved by presenting the mean values of the differences between the relative average bond strength in the database compared to the three models. It is noteworthy that the output from the Castel *et al.* 2016 expression is a reduction factor, applicable to average bond strength. The comparison is made by applying the reduction factor directly to the average bond strength. However, it should be noted that applying this factor to the local bond stress-slip relationship from, say, Model Code 2010 and integrating over the embedment length may lead to different results.

The values obtained from the ARC1990 assessment model are visibly much greater than those from ARC2010. This indicates that ARC1990 gives results that are on the safe side, but which are too conservative when compared to the database. The Castel *et al.* 2016 expression also yields results on the safe side, but not as conservative as ARC1990. On average, the ARC2010 model predicts the capacities better; it yields lower mean residuals for cases with and without stirrups, compared to the other models.

*Table 6: Comparison between mean values of residuals for ARC2010, ARC1990 and Castel et al. 2016 compared to bond database.*

| | ARC2010 | ARC1990 | Castel *et al.*2016 |
|---|---|---|---|
| Without stirrups | 0.05 | 0.30 | 0.12 |
| With stirrups | 0.09 | 0.14 | 0.15 |

## 4.4 Limitations of the model

One important practical limitation is that multi-layer reinforcement is covered by neither ARC1990 nor ARC2010 at this point. However, this is under development for the ARC2010 model. Moreover, the concrete cover is divided into two directions: horizontal and vertical for the newer model, but ARC1990 only deals with cover in one direction. Using the twin-directional covers and confinement coefficient from stirrups allows the location of the main bars in the cross section to be considered in ARC2010.

Representation of possible bond strength increase due to corrosion was considered to be outside the scope of the model. The purpose of this model is to be used in structural assessments of corroded structures in engineering practice. It was chosen not to include possible bond strength increase in the model, mainly due to the following reasons: (i) an assessment of bond capacity is unlikely to be performed before visual signs of corrosion are present (e.g. cover cracking), and at that point the bond is likely to be reduced; (ii) from a practical point of view, a possible increase in bond capacity is not important.

A sensitivity has shown that the average bond strength for cases with stirrups obtained from Model Code 2010, and thus also ARC2010, are sensitive to the clear rib spacing chosen for the reinforcement bars. This is because this parameter determines the slip level at which only the residual bond stress remains. As the clear rib spacing was not specified in most experimental set-ups in the database, an estimated value was used. If this estimation differed from the actual bar properties, this can possibly explain the over-capacity of the ARC2010 model compared to the database results for uncorroded cases, as seen in Figure 13 b). To reduce the influence of the clear rib spacing in the calibration of the ARC2010 model, it was chosen to calibrate the relative capacity reduction due to corrosion rather than the absolute one.

The influence of corroded stirrups on the bond capacity is not explicitly included in the model. However, based on the corrosion level of the stirrups their effective area can be used as input to ARC2010. Furthermore, when corrosion of the stirrups has caused the concrete cover to crack or spall off, this can be treated by using a reduced splitting strength as presented in Section 2.3.2.

The test specimens in the database (and thus the basis of the calibration of the model) were artificially corroded since naturally corroded specimens are very scarce in the literature. The transferability between the effect on bond capacity from artificial corrosion versus natural corrosion is not fully conclusive. Nevertheless, it is the best available data until more specimens with natural corrosion are tested.

Lastly, it should be mentioned that ARC 2010 model has been constructed to produce an average bond strength. An appropriate safety format must therefore be applied to reach the safety requirements of the relevant structural assessment framework.

# 5. CONCLUSIONS AND OUTLOOK

This paper has presented the development of a model to assess the anchorage capacity of corroded steel bars in concrete and is intended for use in engineering practice. The model was calibrated using a large number of bond test results from literature with varying corrosion levels. These were compared to an empirical expression of reduction in bond strength due to corrosion proposed by Castel *et al.* 2016 [48]. Based on the study, the following conclusions can be drawn:

- The ARC2010 assessment model includes confinement effects from concrete and transverse reinforcement, plus the changed confinement effects at the point where corrosion cracks the concrete cover.
- The model represents the physical behaviour well, with a marked decrease in bond strength at the point where corrosion cracks the concrete cover in cases of low stirrup content. The decrease becomes less pronounced for higher stirrup content.
- The incorporation of Model Code 2010 into the assessment model has enabled to account for the reinforcement bar position in the cross section. This was not possible in the previous model. Using Model Code 2010 as the basis for ARC2010 also enables the inclusion of other effects covered in the code, such as transverse stresses and longitudinal cracking.
- ARC2010 gives the full local bond stress-slip curve, rather than just the maximum bond strength or the reduction in anchorage capacity.
- Compared to the previous model ARC1990, the new model shows better agreement with the studied database of bond tests, for cases with and without transverse reinforcement. When normalised average bond strengths from ARC2010 are compared to the bond test database, the average difference is 0.05 for cases without stirrups and 0.09 for cases with stirrups. In other words, ARC2010 predicts slightly lower normalised average bond strengths than those observed in the tests.

Future planned work will be divided into the following parts:

(i) Calibration of modification factors to account for several layers of reinforcement using 3D NLFE analyses.
(ii) Development of a probabilistic ARC2010 model, to incorporate the uncertainties of the basic variables and to enable probabilistic analysis of the response.
(iii) Calibration of modification factors for the deterministic ARC2010 model, for inclusion in the semi-probabilistic safety concepts; in Eurocode for example.

The use of the assessment model will increase the ability of practicing engineers to estimate the anchorage capacity of concrete structures with corroded reinforcement. If the ARC2010 assessment model is used, this will make it possible to keep using more corrosion-damaged concrete bridges.

# ACKNOWLEDGEMENTS

The much-appreciated funding by the Swedish Transport Administration, CBI Swedish Cement and Concrete Research Institute's A-consortium and SBUF is acknowledged.

## REFERENCES


[1] Bell B. Sustainable bridges. D1.3 European Railway Bridge Problems. Report: 2004.

[2] Stewart MG, Wang X, Nguyen MN. Climate change impact and risks of concrete infrastructure deterioration. Eng Struct 2011;33:1326–37.

[3] Almusallam AA, Al-Gahtani AS, Aziz AR, Rasheeduzzafar A. Effects of reinforcement corrosion on bond strength. Constr Build Mater 1996;10:123–9.

[4] Auyeung Y, Balaguru P, Chung L. Bond behavior of corroded reinforcement bars. ACI Struct J 2000;97:214–20.

[5] Cabrera JG, Ghoddoussi P. The effect of reinforcement corrosion on the strength of the steel/concrete "bond." Int. Conf. Bond Concr., Riga, Latvia: CEB; 1992, p. 10/11-10/24.

[6] Al-Sulaimani GJ, Kaleemullah M, Basunbul IA, Rasheeduzzafar. Influence of corrosion and cracking on bond behavior and strength of reinforced concrete members. ACI Struct J 1990;87:220–31.

[7] Rodriguez J, Ortega L, Casal J. Load carrying capacity of concrete structures with corroded reinforcement. Constr Build Mater 1997;11:239–48.

[8] Mangat PS, Elgarf MS. Bond characteristics of corroding reinforcement in concrete beams. Mater Struct 1999;32:89–97.

[9] Berra M, Castellani A, Coronelli D, Zanni S, Zhang G. Steel–concrete bond deterioration due to corrosion: finite-element analysis for different confinement levels. Mag Concr Res 2003;55:237–47.

[10] Almusallam AA. Effect of degree of corrosion on the properties of reinforcing steel bars. Constr Build Mater 2001;15:361–8.

[11] Du YG, Clark LA, Chan AHC. Residual capacity of corroded reinforcing bars. Mag Concr Res 2005;57:135–47.

[12] Fernandez I, Bairán JM, Marí AR. Corrosion effects on the mechanical properties of reinforcing steel bars. Fatigue and sigma-epsilon behavior. Constr Build Mater 2015;101:772–83.

[13] Cairns J, Du Y, Law D. Structural performance of corrosion-damaged concrete beams. Mag Concr Res 2008;60:359–70.

[14] Coronelli D, Hanjari KZ, Lundgren K. Severely Corroded RC with Cover Cracking. J Struct Eng 2013;139:221–32.

[15] Fischer C, Ozbolt J. Influence of bar diameter and concrete cover on bond degradation due to corrosion. Bond Concr 2012 2012:445–51.

[16] Lundgren K, Kettil P, Zandi Hanjari K, Schlune H, Roman ASS. Analytical model for the bond-slip behaviour of corroded ribbed reinforcement. Struct Infrastruct Eng 2012;8:157–69.

[17] CEB. CEB-FIP Model Code 1990. fib Model Code Concr. Struct. 1990, Lausanne, Switzerland: 1993.

[18] Schlune H. Bond of corroded reinforcement - Analytical description of the bond-slip response.

Chalmers University of Technology, M.Sc. Thesis, 2006.

[19] San Roman AS. Bond Behavior of Corroded Reinforcement Bars - FE modelling and parameter study. Chalmers University of Technology, M.Sc. Thesis, 2006.

[20] Perez IF, Tahershamsi M, Marí AR, Lundgren K, Zandi K, Plos M. 1D and 3D analysis of anchorage in naturally corroded specimens. Proc. 10th fib Int. PhD Symp. Civ. Eng. July 21 to 23, 2014, Univ. Laval, Québec, Canada, 2014, p. 547–52.

[21] Zandi K. Corrosion-induced cover spalling and anchorage capacity. Struct Infrastruct Eng 2015;11:1–18.

[22] Lundgren K, Zandi K, Nilsson U. A model for the anchorage of corroded reinforcement : validation and application. Concr. - Innov. Des. fib Symp. Copenhagen May 18-20, 2015, p. 1–11.

[23] CEB. CEB-FIP Model Code 2010. fib Model Code Concr. Struct. 2010, Lausanne, Switzerland: 2013, p. 152–89.

[24] Tahershamsi M, Fernandez I, Zandi K, Lundgren K. Four levels to assess anchorage capacity of corroded reinforcement in concrete. Submitted for publication in Engineering Structures 2016.

[25] Lundgren K. Bond between ribbed bars and concrete. Part 1: Modified model. Mag Concr Res 2005;57:371–82.

[26] Lundgren K. Bond between ribbed bars and concrete. Part 2: The effect of corrosion. Mag Concr Res 2005;57:383–95.

[27] Ožbolt J, Oršanić F, Balabanić G. Modelling processes related to corrosion of reinforcement in concrete: coupled 3D finite element model. Struct Infrastruct Eng 2017;13:135–46. doi:10.1080/15732479.2016.1198400.

[28] Box GEP, Hunter JS, Hunter WG. Statistics for experimenters: design, innovation, and discovery. 2nd ed. Hoboken, New Jersey, USA: Wiley-Interscience; 2005.

[29] Lin H, Zhao Y. Effects of confinements on the bond strength between concrete and corroded steel bars. Constr Build Mater 2016;118:127–38.

[30] Lee HS, Noguchi T, Tomosawa F. Evaluation of the bond properties between concrete and reinforcement as a function of the degree of reinforcement corrosion. Cem Concr Res 2002;32:1313–8.

[31] Shima H. Local bond stress–slip relationship of corroded steel bars embedded in concrete. In: Banthia N, Sakai K, Gjørv OE, editors. Third Int. Conf. Concr. Under Sev. Cond., Vancouver, Canada: 2001, p. 454–62.

[32] Regan PE, Reid ILK. Assessment of concrete structures affected by delamination - 1. Stud Res - Annu Rev Struct Concr Vol 29 2009:245–75.

[33] Zandi Hanjari K, Coronelli D. Anchorage Capacity of Corroded Reinforcement: Eccentric Pull-out Tests. Gothenburg, Sweden, Report 2010:6: 2010.

[34] Coronelli D. Bar corrosion in steel-concrete bond: material and structural effects in R/C. Politecnico di Milano, Ph.D. Thesis, 1998.

[35] Fang C, Lundgren K, Chen L, Zhu C. Corrosion influence on bond in reinforced concrete. Cem Concr Res 2004;34:2159–67.

[36] Coccia S, Imperatore S, Rinaldi Z. Influence of corrosion on the bond strength of steel rebars in concrete. Mater Struct 2016;49:537–51.

[37] Rodriduez J, Ortega LM, Casal J. Corrosion of reinforcing bars and service life of reinforced concrete structures: corrosion and bond deterioration. Int. Conf. "Concrete across borders," Odense, Denmark: 1994, p. 315–26.

[38] Rodriguez J, Ortega LM, Garcia AM. Assessment of structural elements with corroded reinforcement. Int. Conf. Corros. Prot. Steel Concr., Sheffield, UK: 1994, p. 171–85.

[39] Rodriguez J, Ortega LM, Casal J, Diez JM. Corrosion of reinforcement and service life of concrete structures. 7th Int. Conf. Durab. Build. Mater. Components, Stockholm, Sweden: 1996.

[40] Stanish K, R.D. H, Pantazopoulou. Corrosion effects on bond strength in reinforced concrete. ACI Struct J 1999;96:915–21.

[41] Horrigmoe G, Saether I, Antonsen R, Arntsen B. Sustainable Bridges. Laboratory investigations of steel bar corrosion in concrete - background document SB3.10. Report: 2007.

[42] Law DW, Tang D, Molyneaux TKC, Gravina R. Impact of crack width on bond: confined and unconfined rebar. Mater Struct 2011;44:1287–96.

[43] Ng S, Craig BC, Soudki KA. Effects of FRP wrapping on the bond strength of corroded steel reinforcing bars. 2nd Mater. Spec. Conf. Can. Soc. Civ. Eng., Montreal, Canada: 2002, p. 1–9.

[44] Ghandehari M, Zulli M, Shah SP. Influence of corrosion on bond degradation in reinforced concrete. Proc. EM2000, Fourteenth Eng. Mech. Conf., Austin, Texas: ASCE; 2000, p. 1–15.

[45] Orangun CO, Jirsa JO, Breen JE. A Reevaluation of test data on development length and splices. ACI Struct J 1977;74:114–22.

[46] Mancini G, Tondolo F. Effect of bond degradation due to corrosion - A literature survey. Struct Concr 2014;15:408–18.

[47] The MathWorks Inc. MATLAB R2015b 2015.

[48] Castel A, Khan I, Francois R, Gilbert RI. Modeling steel concrete bond strength reduction due to corrosion. ACI Struct J 2016;113:973–82.

[49] Prieto M, Tanner P, Andrade C. Multiple linear regression model for the assessment of bond strength in corroded and non-corroded steel bars in structural concrete. Mater Struct 2016;49:4749–63.

[50] Berrocal CG, Fernandez I, Lundgren K, Löfgren I. Corrosion-induced cracking and behaviour of corroded reinforcement bars in SFRC. Compos Part B 2017;113:123–37.